Adaptive Flight Control System

Mr. S. S. Osder, Sperry Gyroscope Company

INTRODUCTION

This paper presents a summary of research and development accomplished on a program to evaluate the feasibility of an adaptive automatic flight control system under Contract AF 33(616)-5075. The work was performed from May 1957 to May 1958, for the United States Air Force, Wright Air Development Center, Wright-Patterson Air Force Base, Ohio by the Aeronautical Equipment Division of the Sperry Gyroscope Company, Division of Sperry Rand Corporation, Great Neck, New York. The system investigated employs so-called optimum response models in the control system forward loop and uses linear and non-linear techniques to force the controlled vehicle to execute maneuvers with minimum error from the response dictated by the model. The stability problems associated with these high gain control techniques are alleviated by means of a Performance Computer which continuously detects stability boundaries and adjusts automatic flight control system gains to within a desired margin of these boundaries. The required adjustments are determined by extracting the essential information from the vehicle-autopilot closed loop impulse response. Periodic low amplitude excitation impulses below the human pilot' s detectable threshold are applied to the system with the Performance Computer establishing the required adjustments on the basis of monitored response. Adaptive stabilization and maneuvering configurations for a variety of vehicles were obtained in analog computer studies which included actual physical equipment mock-ups. The Performance Computer was also used to provide automatic cross-over between reaction jet and aerodynamic controls during exit and re-entry maneuvers. A complete description of the Sperry adaptive flight control system program for the Air Force is reported in the following documents prepared for WADC on Contract AF 33(616)-5075.

1. First Interim Technical Report - Feasibility Study-Automatic Optimizing Stabilization System, S. S. Osder; Sperry Report No. 3265-3683, September 1957.

2. Second Interim Technical Report - Feasibility Study-Automatic Optimizing Stabilization System, S. S. Osder, I. N. Hutchinson; Sperry Report No. 3265-3702, November 1957.

3. Third Interim Technical Report - Feasibility Study-Automatic Optimizing Stabilization System, S. S. Osder, I. N. Hutchinson; Sperry Report No. 3265-3733, February 1958 (Confidential)

4. Final Technical Report - Feasibility Study-Automatic Optimizing

Stabilization System, S. S. Osder, I. N. Hutchinson; Part I and II Contract No. AF 33(616)-5075, Sperry Report No. 3265-3746, WADC TR 58-243, ASTIA Document No. AD 155576, June 1958.

DISCUSSION

The system investigated employs three basic adaptive techniques aimed at providing optimum performance throughout the complete range of rapidly varying flight conditions. These techniques may be classified as:

1. Passive adaptation by virtue of linear feedbacks around an optimum response model.

2. Alteration of controller structure as a function of measured performance by means of non-linear modification of system input signals.

3. Measurement of the critical part of the closed loop impulse response and adjustment of controller parameters as a function of this measurement.

Before describing the manner in which these techniques are employed, it would be valuable to elaborate somewhat on the philosophy behind the classifications.

a. Passive Adaptation by Linear Feedback - Consider first the passive adaptation which is an inherent property of every system with negative feedback. This is easily demonstrated by the control system block diagram illustrated by figure 1. The dynamic element being controlled, H_A, may be an airplane transfer function which relates the aircraft's attitude with the input moments represented by X_d and X_c. The moment X_d is an external disturbance such as may be caused by a gust induced variation in lift. If the control loop represented by the controller H_1 is not closed, the aircraft's response to the disturbance will be given by

$$\left[\frac{\Theta_o}{X_d} \right]_{\substack{\text{Open} \\ \text{Loop}}} = H_A \qquad (1)$$

where H_A is defined by the combination of aerodynamic and inertial forces acting on the aircraft.

Now, if we close the loop containing the controller H_1, the output response to the same disturbance, X_d becomes

$$\left[\frac{\Theta_o}{X_d}\right]_{\substack{\text{Closed}\\ \text{Loop}}} = \frac{H_A}{1 + H_1 H_A} \qquad (2)$$

If $H_1 H_A > 1.0$

$$\left[\frac{\Theta_o}{X_d}\right]_{\substack{\text{Closed}\\ \text{Loop}}} \approx \frac{1}{H_1} \qquad (3)$$

which is the result to be expected in any application of negative feedback. But, the implications of equation (3) are very intriguing when adaptive performance is being sought. This equation states that the controlled aircraft's response to the disturbance will be independent of the aircraft. Thus the aircraft can fly through any altitude and Mach number regime, or even transform itself from a heavy low speed transport to a hypersonic vehicle, but the response will remain constant, determined only by the controller transfer function. This is obviously as adaptive as a control system can get, and no complex array of computing equipment is required. However, as practical designers of automatic flight control systems will readily testify, so remarkable a controller as the H_1 of equation (3) cannot in general be achieved with physically realizable equipment. Practical limitations are imposed by the finite attainable servo bandwidths and the effects of control system non-linearities. Nevertheless, in many instances, it is possible to attain a fairly good approximation of the desired H_1. This compromise value of H_1 can be employed to greatest advantage when the autopilot design incorporates an optimum response model and the so-called conditional feedback technique. In effect, this technique permits us to use information contained in the input signal to maximum advantage in minimizing dynamic errors from the desired response.

b. Optimum Response Model - The optimum response model technique can be used to make the system's response to commands independent of the system's response to disturbances. Figure 2 is a block diagram which illustrates a flight control loop with conditional feedback around an optimum response model. The essential difference between figures 1 and 2 is the utilization of a model which will shape the command to represent desired performance. This is compared to actual performance, resulting in generation of an error, ϵ which is further operated on by the conditional feedback block.

The arrangement of a block diagram to show a conditional feedback loop based on a performance model is an illustration of a manipulation of system block diagrams, aimed at showing adaptation capability of virtue of linear feedback. It is emphasized that the use of the model concept

does not by itself represent any fundamental advance in servomechanism art. It is, in reality, no more than a rearrangement of the conventional servomechanism block diagram. To illustrate, the diagram of figure 2 can be easily redrawn into its single loop equivalent as indicated in figure 3. All that has happened is that a pre-filter $[1 + g(s)]$ has been inserted into the command path.

Representing the system block diagram to incorporate an optimum response model emphasizes a very important design concept which points the way toward the attainment of an adaptive capability. This concept involves a design which permits the separation of command and disturbance response. Such a separation permits the over damping of the aircraft autopilot closed loop disturbance response without compromising the response to commands. This principle can be demonstrated by the following simplified illustration. Consider first the representation of the control block diagram incorporating a model as shown on figure 2. The conditional feedback in this figure is the error signal which represents the difference between the actual and the desired response to the command, Θ_i. This block diagram can of course be redrawn to show the model as a pre-filter on the command as illustrated in figure 3.

Equation 3 described the response to a disturbance, X_d, showing that it approaches dependence upon only the controller transfer function, H_1. However, from figure 3 it is seen that the response to the command Θ_i is defined by

$$\frac{\Theta_o}{\Theta_i} = \frac{g'(s)\ H_1(s)\ H_A(s)}{1 + H_1(s)\ H_A(s)} \qquad (4)$$

Again if $H_1(s)\ H_A(s) > 1$

$$\frac{\Theta_o}{\Theta_i} \approx g'(s) \qquad (5)$$

which states that the response to the command Θ_i is defined only by the pre-filter (or model) transfer function. The first step, therefore, toward designing an automatic flight control system which displays an inherent adaptive capability is to define the optimum response model. This turns out to be a rather simple task since the optimum response model for an attitude command is a first order lag while the optimum response model for an attitude rate command such as a pilot's stick force input is an integrator preceded by a first order filter.

c. Non-Linear Modification of Controller Structure - The next problem which must be overcome in our quest for adaptive performance relates to our ability to maintqin H_1 (s) H_A (s) greater than 1.0 so that equation (5) can be obtained from equation (4). Studies of aircraft dynamic variations encountered throughout a typical flight regime indicate that in some instances a single set of autopilot gains can provide nearly constant airplane-autopilot dynamics over a complete subsonic and supersonic range of flight conditions. However, in most cases a single set of gains represents too severe a compromise in performance so that the objective of keeping H_1 (s) H_A(s) greater than 1.0 for most of the flight regime cannot be met. The critical factor in the aircraft dynamic change which necessitates a reduced autopilot aircraft combination gain is the approach of the aircraft natural frequency to the bandwidth of the control system (including sensors and actuators). The adaptive system described in this paper will automatically detect the requirement that autopilot gain must be reduced at these critical flight conditions. However, the " non-linear" modification of controller structure effectively compensates for the reduced linear system gains by making the system respond as though its gains were several times higher than the linear gain parameters would imply. Thus, the use of a non-linear controller permits the criterion of H_1 (s) H_A (s) > 1.0 to be maintained even when linear stability considerations force the gain of H_1 (s) to be lowered below the minimum value required for a linear adaptive configuration.

d. Impulse Response Measurement - It remains, then, to discuss the method by which the autopilot gain is raised or lowered to reflect the maximum gain restrictions imposed by the controller bandwidth limitations at the various flight conditions. The technique employed is based on the extraction of required gain adjustment data from the aircraft -autopilot closed loop impulse response. Many methods for obtaining the impulse response of an unknown dynamic element have appeared in the recent servo-mechanisms literature. These methods, however, involve fairly complex equipment since they employ such techniques as sampling and storage of a transient' s past history and correlation function computations. Complexity of this nature would be unavoidable if we attempted in-flight measurement of a completely unknown dynamic element. This, however, is not true in the case of an airplane transfer function. Since we know the basic form of the aircraft' s equation of motion, we also know the general form of the transfer function H_A(s) discussed previously. That is, we can always approach the problem with some qualitative knowledge of the poles and zeros of H_A (s) even when we possess no information relating to the specific coefficients of the aircraft' s equations of motion. From this vantage point of knowledge rather than ignorance of the controlled element, we can extract the required specific details without resorting to complex computations. In the following disucssion it will be shown that a relatively simple measurement can provide the necessary inputs to the gain adjusting circuitry. Moreover, it will be shown that this

measurement always remains independent of the automatic flight control loop in that the required equipment may be inserted or removed without disturbing the basic autopilot. Thus, the gain adjusting system which is referred to hereafter as the Performance Computer need be incorporated only in those applications where the first two adaptive techniques cannot adequately cope with the variations in vehicle dynamics.

c. Performance Computer - Before describing the operation of the Performance Computer, it is important to review the nature of the stability problem which this computer must control. This can be determined with the help of figure 4 which is applicable to the pitch control system. The system stability can be determined from the open loop transfer function $H_1 H_S H$. Consider H_1 to be a simple rate plus displacement autopilot given by the following transfer function.

$$H_1(s)\, H_S(s) = K \left[1 + K_R\, s\right] \quad H_S\,(s)$$

where K is the static gain in degrees of surface per degree of attitude error, K_R is the ratio of rate to displacement gain and H_S represents the dynamics of the servo actuator transfer function. $H_A(s)$, the rigid airplane transfer function may be described for the case of pitch control as

$$H_A(s) = \frac{\Theta}{-\delta_E} = K_A \frac{\left(\frac{s}{\omega_1} + 1\right)\left(\frac{s}{\omega_2} + 1\right)}{\left(\frac{s^2}{\omega_{A^2}} + \frac{2\zeta_A s}{\omega_A} + 1\right)\left(\frac{s^2}{\omega_B^2} + \frac{2\zeta_B s}{\omega_B} + 1\right)} \qquad (6)$$

where K_A is the airplane gain, a quantity dependent upon a large number of aerodynamic factors, but in the short period control frequencies it is primarily determined by surface effectiveness, longitudinal moment of inertia and static stability. It is important to note that K_A has the identical effect as autopilot gain K on the open loop transfer function $H_1 H_S H_A$. In the ideal case, the variation of K_A with flight condition is completely defined so that an open loop gain schedule can be used to change the autopilot gain and thereby permit the combination KK_A to produce the desired closed loop characteristics. The problem of the adaptive autopilot involves situations in which we cannot predict K_A.

The poles of equation (6) are defined by ω_A and ζ_A the phugoid natural frequency and damping ratio, and ω_B and ζ_B the airplane short period natural frequency and damping ratio. The zeros ω_1 and ω_2 are associated with two of the airplane response time constants. The flight path angle initial response time constant to a pitch angle change is defined by ω_1 and ω_2 defines the time constant of the flight path angle as it decays to

its steady state value after the initial response. Figure 5 shows the complete root locus of figure 4 with H_s neglected. Note that there is no stability problem indicated by figure 5 since the open loop poles traverse no region of poor stability as they move toward the open loop zeros. This root locus is another way of illustrating how the autopilot can completely dominate the dynamics of the closed loop response since it demonstrates how the autopilot zero at $-\frac{1}{K_R}$ becomes the dominant pole of the closed loop system as the autopilot gain approaches infinity. Actually, a realistic gain of K = 2 to 3 is often sufficient to move the airplane short period pole 98% of the distance on the S plane to the terminating zero. Now let us consider the effect on this root locus when we include the servo dynamics, H_s. Consider first, second and third order servo dynamics defined by:

1. 1st order servo $H_s = \dfrac{1}{\frac{s}{\omega_{s_1}} + 1}$

2. 2nd order servo $H_s = \dfrac{1}{\frac{s^2}{\omega_{s_2}^2} + \frac{2\zeta_s s}{\omega_{s_2}} + 1}$

3. 3rd order servo $H_s = \dfrac{1}{\left(\frac{s}{\omega_{s_1}} + 1\right)\left(\frac{s}{\omega_{s_2}^2} + \frac{2\zeta_s s}{\omega_{s_2}} + 1\right)}$

The form of the root loci when these three servos are included is shown in figures 6, 7, and 8. In all three cases, a new high frequency problem area is introduced, for in the previous ideal case represented by figure 5, an increase in gain always moved roots toward a higher damping region. The gain K at which these new servo loci cross the imaginary axis corresponds to the gain margin of the stabilization system. Figure 9 shows a family of curves for the loci of second order servo roots with different servo system natural frequencies. These curves demonstrate the well known technique of increasing the system gain margin by expanding the servo bandwidth, for the value of gain required to cross the imaginary axis increases with the servo natural frequency.

The important point being made in figures 6, 7 and 8 is that the only type of instability which can appear in an overdamped pitch stabilization system is a high frequency instability related to the control system bandwidth. It is noted that the dynamic lags identified with the actuator transfer function H_s could just as well be considered part of any other dynamic lag introduced in the open loop $H_1 H_s H_A$. This would apply to the gyroscopic sensors or the autopilot computing networks. The primary concept involved in the stabilization system under study in this program is the automatic detection and restraint to within stable boundaries of these " high frequency" roots. A monitoring system which can hold these roots within an acceptable margin from the right half plane will automatically set the system gain at the maximum attainable value.

It is important to emphasize that the " high frequency" roots are the

only limitations to system gain margin. Gain margin is defined as that value of K which will cause a cross-over of the " high frequency" roots into the right half plane. This reasoning is applicable to types of pitch stabilization configurations other than those illustrated by the root loci of figures 6, 7, and 8. For example, it applies to systems such as those which employ second derivative pitch data and integrating servos as in figure 10. Moreover, a similar analysis can demonstrate that this same principle is applicable to aircraft roll and yaw attitude control systems. It is noted, however, that the attitude control systems must employ displacement references and must command aircraft moments in those axes about which the attitude displacement errors appear if we wish to use the high frequency instability as a performance criterion. Thus, roll attitude errors must be corrected by commanding yawing induced rolling moments and heading errors corrected by commanding yawing moments. In control configurations which act as dampers only (rate autopilots) the high frequency instability discussed above will appear but other types of oscillations may develop before the high frequency roots pose a stability problem. For example, a yaw damper has an optimum gain, and any increase in gain above this value can lead to a decrease in lateral stability at periods several times greater than the " stick fixed" dutch roll period.

Figure 11 is a block diagram illustrating the technique employed for bounding the critical high frequency roots within a range of acceptable damping ratios. The control system is excited by a combination of the attitude control signal and the small amplitude narrow pulses inserted at the servo actuator input. Because of the orientation of the poles and zeros of the aircraft-attitude control system combination, only the oscillatory mode associated with the high frequency servo roots will be excited by a small amplitude impulse. It is noted that if we wished to measure the complete impulse response of the closed loop airplane-autopilot combination, we could measure the airplane response rather than the actuator response. However, if we wished to detect the influence of all the poles and zeros inherent in the equation of the airplane-autopilot closed loop transfer function, we would have to use an excitation impulse many times larger than the one required to excite only the critical high frequency pole pair.

The system illustrated in figure 11 measures the response δ_E to a pulse δ and shapes this response to a series of fixed amplitude pulses. The number of these output pulses is a measure of the number of reversals of δ_E in response to the excitation impulse and therefore is proportional to the damping ratio of the " high frequency" roots. The logic circuitry establishes the criteria for autopilot gain changes as a function of an excess in output pulses during a given sampling period. The sampling period and the excitation pulse shape and amplitude are established in the excitation and sequence control. The logic circuits establish the boundaries of acceptable damping ratios of the critical " high frequency" roots. The combination of the Sequence Control, logic circuitry, pulse shaper and counter are referred

to as the Performance Computer.

The performance computer' s function is to automatically seek the maximum attainable gain within the specified stability limits. By operating the autopilot at its maximum permissible level we always operate with a stabilization configuration which gives the closest approximation to the attainment of complete adaptation as defined by equations 3 and 5. The performance computer generates the periodic pulses which are used to probe the aircraft' s environment. In general, the rate of pulsing can be made a crude function of the rate of change of the aerodynamic environment. The pulse rate was slowed down when conditions were static, and automatically accelerated when the aerodynamic static and dynamic pressures changed. In the case of missiles or reentry research vehicles this sophistication need not be used. Actually, no additional circuitry is required in the excitation and sequence control for this variable pulse rate function since the basic timing flip-flop is designed to increase frequency as a function of a voltage (ac or dc) which represents the rate of change of the flight environment.

Figure 12, then, is a comprehensive block diagram of the adaptive configuration which was evaluated in extensive simulator studies which utilized actual hardware such as servo amplifiers, hydraulic actuators and a breadboard Performance Computer.

f. Performance Computer Implementation - The circuitry required to implement the performance computer function was relatively simple and noncritical. In the breadboard system build on Air Force Contract AF 33(616)-5075, the logic circuits employed electro-mechanical relays to control the speed and direction of the gain adjusting motor. These relays represented a complexity and weight penalty which can easily be eliminated with semiconductor switching devices. The relays were used in the breadboard system because they provided a valuable flexibility which permitted changes to the logic system with a minimum of circuit modifications.

A logic diagram of the performance computer is shown on figure 13. The system operates by inserting impulses into the automatic pilot at controlled intervals and monitoring the control surface response. Any oscillatory motions of the actuator output will be converted into a train of pulses and counted in a decade counter. In the breadboard version, a magnetron beam switching tube was used as the counter. Part of a conventional decade counter constructed of three flip-flops can provide improved reliability for this function and thus may be used in place of the beam switching tube. It is noted that the simplest type of binary element is required for this counting function so that the more elaborate circuitry associated with high speed, transistorized flip-flops need not be used.

The number of counts detected at the decade counter will depend upon the number of surface reversals which exceed the threshold sensitivity of the

Schmitt Trigger and therefore, will be a measure of the critical root damping ratios. The beam switching tube counter shown on figure 13 was used to operate relays which dictate the direction and speed of the automatic pilot gain control motor. The circuitry was arranged to give a slow decrease in gain for a count of three, a medium speed decrease in gain for a count of four and a fast decrease for a count of five. A slow increase in gain occurs the second time a count of less than two is obtained. This logic is included in order to prevent a gain increase when a higher count is expected. When a count of two is obtained, the performance computer' s criterion for correct autopilot gain is satisfied and no change occurs. It is again noted that the relays could be eliminated by employing a direct read-out from the counter circuit to actuate transistor gates which would vary the speed and direction of the gain control motor.

Figure 14 is a block diagram of the sequence and excitation control portion of the logic diagram presented in figure 13. The period of the astable multivibrator is controllable in the range 3 to 30 seconds by a low power 400 cycle control voltage. Each cycle of this astable binary circuit causes one 3 second pulse to be generated in the monostable binary. A test impulse is formed and sent to the automatic pilot at the beginning of this three second pulse and the counter and motor gates are opened to permit detection and correction of non-optimum gain. The counter and motor gates are closed at the end of the three second pulse to prevent gain changes due to random disturbances, and the counter is reset to zero to prepare for the next test period. This sequence control arrangement could be improved by the inclusion of an additional monostable binary to close the counter gate sooner than the motor gate. Since the critical frequency will generally be higher than three cycles per second, the critical root damping ratio can be determined in a half second and this modification would minimize the possibility of false high counts due to extraneous noise.

The excitation and sequence control circuits could be common for all aircraft axes. The counter and gain control logic circuit must be repeated for the pitch and roll axes. The entire performance computer function for pitch and lateral control can be packaged in a volume of 40 to 50 cubic inches and is presently envisioned as a plug-in module of a complete AFCS.

g. Typical System Performance in Supersonic Aircraft - Before showing results which demonstrate system performance obtained with the above configuration, some mention should be made of techniques other than the excitation impulse as a means of deriving the required information about the closed loop impulse response. At the start of the program, it was suspected that atmospheric turbulence might provide an adequate excitation to the system without requiring the addition of an impulse. This did not prove to be feasible because the random nature of this type of disturbance could not provide consistent signals to the Performance Computer. It was found that when the gust disturbances did not cause an adequate surface response for a few

sampling intervals, the stability boundaries were temporarily exceeded and divergent high frequency oscillations began to develop. These oscillations were eventually bounded and damped, but unlike the performance obtained with the periodic impulse, the instability actually reached the point of divergence. Figure 15 is a computer record which illustrates the erratic performance obtained with excitation derived from atmospheric turbulence only.

A typical demonstration of the system's capability is illustrated by the recording on figure 16. Here a supersonic airplane which experiences a severe change in dynamics is decelerated and accelerated at constant altitude so that the range from Mach=1.6 to Mach=0.4 is covered. The aircraft's pitch natural frequency varies from about 13 radians per second at the high speed condition to about 2 radians per second at Mach 0.4. In figure 16, the impulse period is seen to vary from 21 seconds to 3 seconds as the deceleration increases. During the deceleration, the Performance Computer tracks the maximum permissible gain through a range of 1.0 to 3.5 and maintains the critical root damping ratio within acceptable bounds. At the start of the acceleration phase of the maneuver, the critical root damping ratio falls temporarily below desirable levels due to non-optimum gain control motor speeds. This difficulty could easily be alleviated with the use of a gain control motor having improved speed characteristics. It is seen, however, that the performance computer recovers rapidly and develops the allowable maximum gain throughout the rest of the maneuver.

In the following recordings which illustrate maneuvering performance with an F-104A airplane, the characteristics of the non-linear control in the adaptive autopilot forward loop were dictated by specific parameters of the hydraulic actuator used. For example, this actuator's authority limits of ± 5 degrees prevented an even more effective utilization of the non-linear gain controls since the actuator was effectively employed as a dual mode controller; that is proportional control for small errors and "bang-bang" control for large errors. For the authority limits available, no further improvement could be obtained by raising the gain of the non-linear channel, although in general, a considerable increase in gain above the value used could be attained before an amplitude sensitive limit cycle would occur. It is noted that several methods of non-linear error gain control were investigated before the configuration eventually used was selected. All combinations of variable gains and gain switching of the rate and displacement signal as a function of the absolute value of the error and error rate were investigated. Fortunately, the technique which gave the best results was also the simplest to implement. This technique varies the displacement gain only, and the gain increase is a simple function of the absolute value of the displacement error. Its effect is that of superimposing a "bang-bang" controller on a linear proportional control system. For the parameters used, an attitude error of greater than about 1.0 degree would command maximum surface deflection so that the aircraft is constrained to follow a commanded reference with extreme tightness even when stability consideration force a reduction in linear system gains. Figure 17 is a

plot of the surface deflection versus pitch error for the linear and non-linear system at Mach 0.6, 0.95 and 1.6. flight conditions of the F-104A. Note that the linear system gains at these different flight conditions are those which were automatically set by the Performance Computer. It is apparent from this figure that the non-linear system is extremely effective in minimizing the actual difference between the control action at the different flight conditions. Its effect is to minimize the possibility of ineffective control because of reduced autopilot gain at flight condition III. It is noted that in that particular case, the autopilot gain was reduced by the Performance Computer not because the aircraft surface effectiveness increased but primarily because the limited control system bandwidth could not cope as effectively with the increased aircraft natural frequency.

Figures 18, 19, 20, 21, and 22 are typical analog computer recordings illustrating pitch rate maneuver performance. It is noted that in these recordings, command error rates are not employed so that the effectiveness of the non-linear error gain controls can be seen more clearly. The aircraft is an F-104A at 25,000 feet and various Mach numbers. In each case, the input is a step pitch rate command. Figure 18 shows the response when the non-linear controls are not used. The command is equivalent to 2.0 incremental " g" steady state when airspeed changes are neglected. The second maneuver on this figure differs from the first in that g-limits of ± 1.0 g' s are set by the g-limiter. It is noted that the g-limiter gains exceed those which would be feasible if linear signal techniques are employed and the response is sharper than can be obtained with passive cut-off methods. In this implementation, a signal proportional to the excess in g' s is applied to the pitch control system only when the g-limit has been exceeded. Since extremely high gains on the g-error signal are employed, the immediate effect is a large correction in the direction to lower the pitch rate to that value corresponding to the limit g' s.

It is seen from figure 18 that when the non-linear pitch error gains are not used, the instantaneous pitch error reaches as high as 3.0 degrees and there is a slight overshoot in the g-limit. On figure 19 the non-linear gain control is employed and the maximum instantaneous pitch error is limited to one degree. Also, the g-limiting is sharper. Note that the excitation impulse is always present although on figures 18 and 19 its effect cannot be seen in the pitch rate response.

Figure 20 shows the same maneuver as in figure 19 but with mild atmospheric turbulence present. It is seen that the effect of the turbulence would easily be enough to mask any manifestations of the excitation impulse as far as a human pilot would be concerned. Figures 21 and 22 are similar maneuvers at Mach 0.60 and 1.6 where the autopilot gain has been set by the performance computer to about twice and one half the value it set for the previous flight condition. In figures 21 and 22 the effects of turbulence are also illustrated. These recordings show that in mild turbulence any trace of the excitation impulse is completely masked by the gust disturbances. Also, note that the

performance computer is able to discriminate between the surface activity due to the turbulence and the activity resulting from the excitation impulse. Extensive tests on the effects of turbulence on the performance computer have shown that turbulence will cause the performance computer to lower the autopilot gain only about 1.0 to 2.0 DB. To an extent, this slightly lower gain may actually be a desirable characteristic.

h. Application to Space Vehicle Exit and Re-Entry Control Problem

A logical extension of the maximum gain seeking automatic control system is the application to high speed vehicles which perform both inside and outside of the atmosphere. This can be appreciated if we recall that the true automatic pilot gain is a combination of the system gain and surface effectiveness. In order to maintain effective attitude control, the system gain must increase as the surface effectiveness decreases. As the vehicle departs from the atmosphere, the surface effectiveness decreases to zero and the required aerodynamic automatic pilot system gain approaches infinity. Since the maximum gain seeking function of the Performance Computer will automatically try to compensate for the loss in surface effectiveness, automatic switching to reaction-jet attitude control can be obtained when the aerodynamic automatic pilot system gain reaches some specified high value. The following is a description of some of the results obtained when the Performance Computer was used to provide cross-over of aerodynamic and reaction-jet controls during exit and re-entry maneuvers of a hypothetical ballistic-glide vehicle.

The trajectory simulated on the analog computing equipment involved an initial drop at 38,000 feet at Mach 0.5, an acceleration for 80 seconds to Mach 6.0 with an eventual climb to 260,000 feet, and a ballistic descent with leveling and deceleration at about 90,000 feet. Figure 23 shows the uncontrolled vehicle response during this exit and re-entry maneuver. The vehicle was excited by a short moment pulse during the exit phase. The apparent divergence in the oscillatory amplitude as the frequency decreases is characteristic of a spring-mass oscillatory system in which the spring stiffness decreases with time.

Figure 24 shows the response to 2-degree step pitch commands during an exit maneuver with only the aerodynamic automatic pilot operating. Note the periodic impulses appearing at the control surface and the aerodynamic autopilot gain decreasing in response to the initial vehicle acceleration and then increasing as the surface effectiveness diminishes toward zero. Figure 24 shows that despite the Performance Computer's increase in the autopilot static gain to 10.0, an attitude command causes an uncontrolled tumbling of the aircraft as the air density approaches zero.

Figure 25 shows the response to 2-degree step pitch commands during an exit maneuver with only the jet reaction automatic pilot operating. This record shows that the jet reaction automatic pilot contributes little in the way of stabilization during the first 30 seconds of the maneuver, and

does not provide a very effective attitude control for another 20 seconds. Figure 26 shows the vehicle attitude stabilization response during exit and re-entry maneuvers with the combined system in operation. A reaction jet crossover switch was located on the output shaft of the Performance Computer's gain adjuster. This switch was set to cut-in reaction jet control when the automatic pilot static gain was driven to a value of 6.0. The recording on figure 26 shows that tight attitude control and good stability margins were thereby maintained at all times during the exit and re-entry. Figure 27 shows a re-entry which includes a rapid trim change equivalent to five degrees of control surface deflection in four seconds. The maximum disturbance in attitude is seen to be less than 0.25 degrees. The Performance Computer and its associated excitation impulses thus act to probe an unknown environment and establish the optimum control configuration on the basis of interaction between the aerodynamic forces and the control system response.

SUMMARY

In summary, we have described an approach to the development of an adaptive automatic flight control system which uses as a starting point the inherent adaptation obtainable from a high gain control system employing linear feedbacks around an optimum response model.

The linear system was augmented by a simple non-linear control of the error signal to give the effect of a " bang-bang" controller superimposed on a proportional control system. This non-linear augmentation expanded the inherent adaptive properties of the linear configuration. The limitations of the linear system were shown to be a function of the control system bandwidth with the upper bounds on the linear system gain dictated always by a pair of complex conjugate high frequency poles in the closed loop transfer function. A method of bounding these critical roots within a region of acceptable damping ratios by means of a fairly simple measurement of the system's response to a small excitation impulse was shown to be feasible. The feasibility of this technique was established on the basis of extensive analog computer studies in real time simulations of various control problems employing realistic physical equipment mock-ups. The actual hardware used included a multiple input hydraulic actuator with associated servo amplifier circuitry and a bread-board Performance Computer which measured the critical part of the system's closed loop impulse response. The required magnitude of the periodic excitation impulses was in general below the human pilot's detectable threshold and it was demonstrated that it should definitely be undetectable to a pilot in any of its manifestations if a slight amount of turbulence is present.

These techniques were applied with considerable success in the simulator studies to both supersonic aircraft displaying severe dynamic changes over a wide range of flight conditions and a rocket powered hypersonic vehicle in planetary atmosphere exit and re-entry maneuvers. In general, it was concluded that the straightforward linear system with the optimum response models

augmented by the simple non-linear control element could provide an attitude stabilization system displaying constant dynamics for some transonic and supersonic aircraft without requiring gain scheduling. However, in the case of vehicles which undergo extreme changes in dynamics, the Performance Computer and its associated excitation impulses could be used to automatically set the optimum automatic pilot gain throughout any range of flight conditions. An especially significant application of the Performance Computer's continuous probing of an unknown environment was demonstrated in its use as a means for providing the automatic crossover of aerodynamic surface and reaction jet controls during space vehicle exit and re-entry maneuvers.

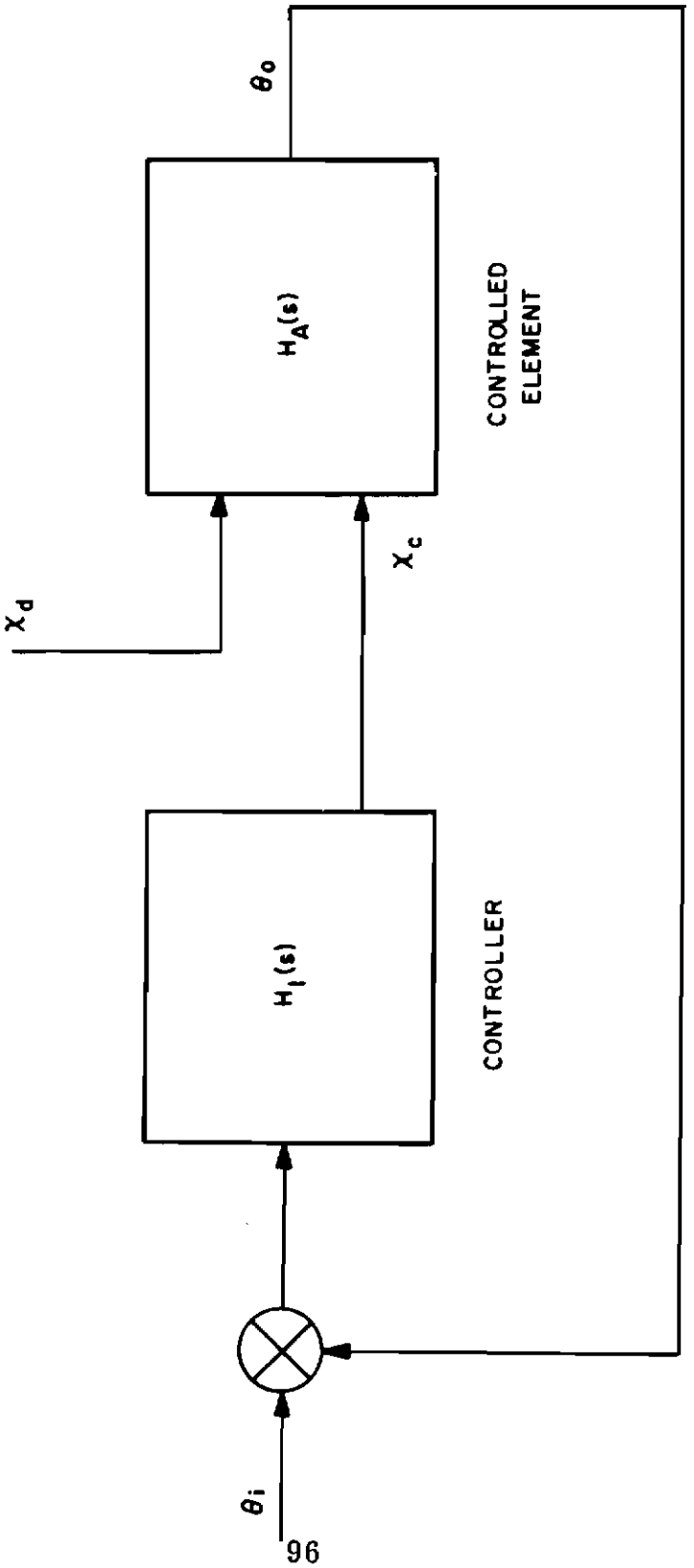

Fig 1 BASIC CONTROL BLOCK DIAGRAM

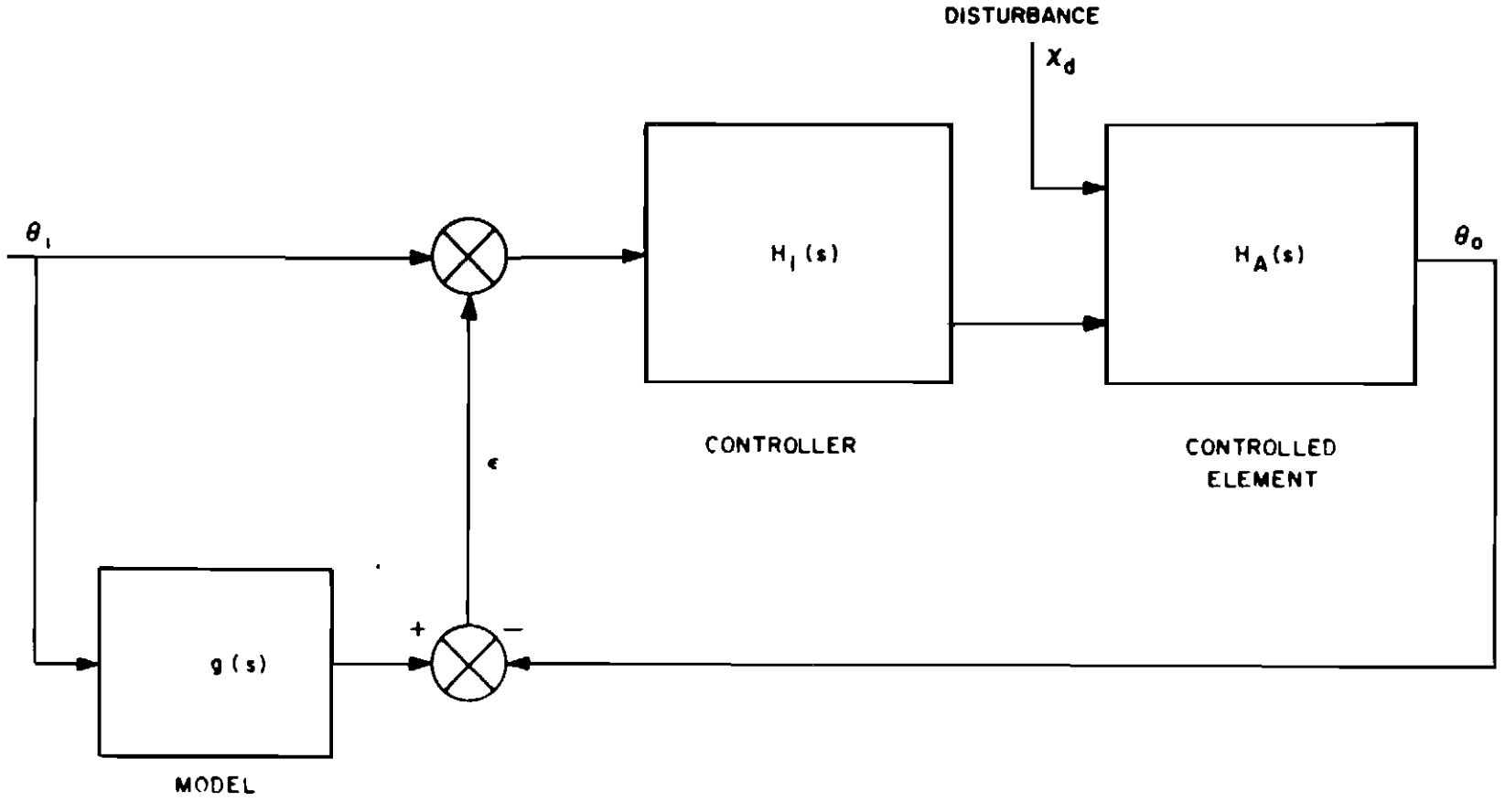

Fig 2

CONTROL BLOCK DIAGRAM
WITH CONDITIONAL FEEDBACK

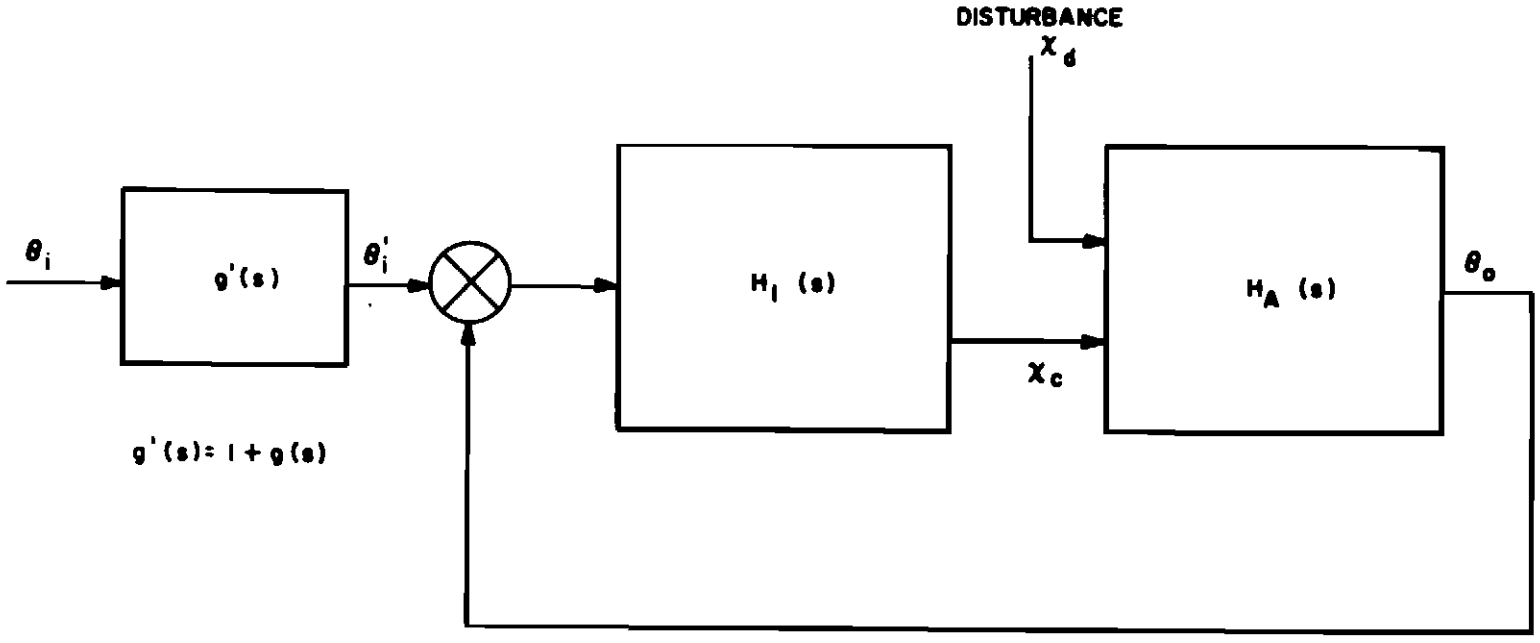

Fig 3

EQUIVALENCE OF
CONDITIONAL FEEDBACK CONFIGURATION
AND CONVENTIONAL SYSTEM
WITH PRE-FILTER

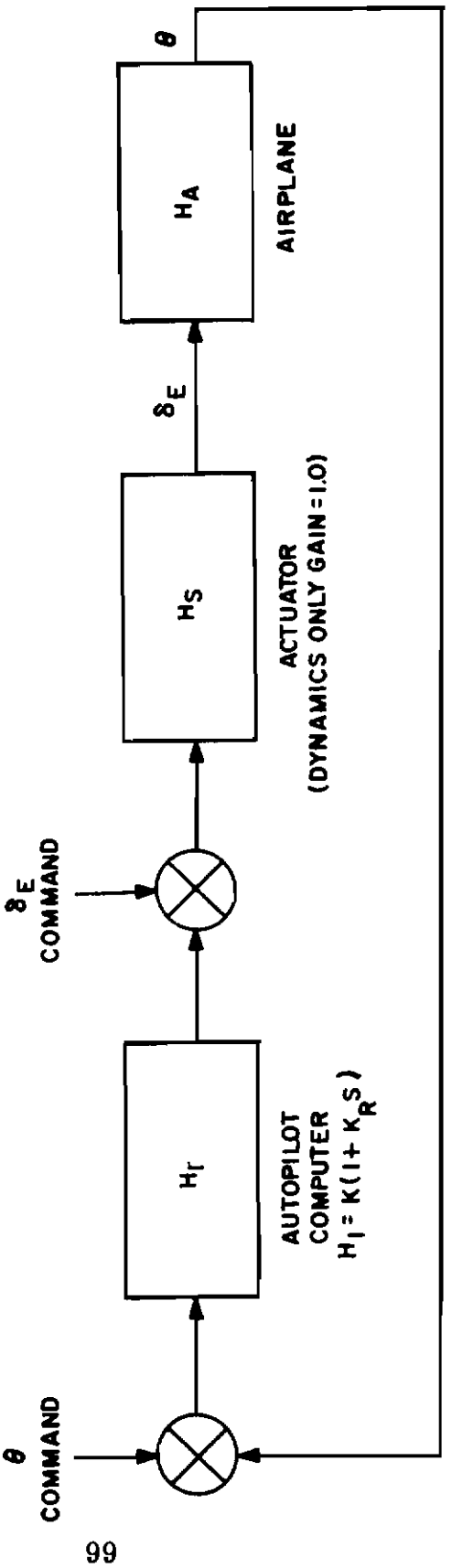

BASIC PITCH ATTITUDE STABILIZATION SYSTEM

Fig 4

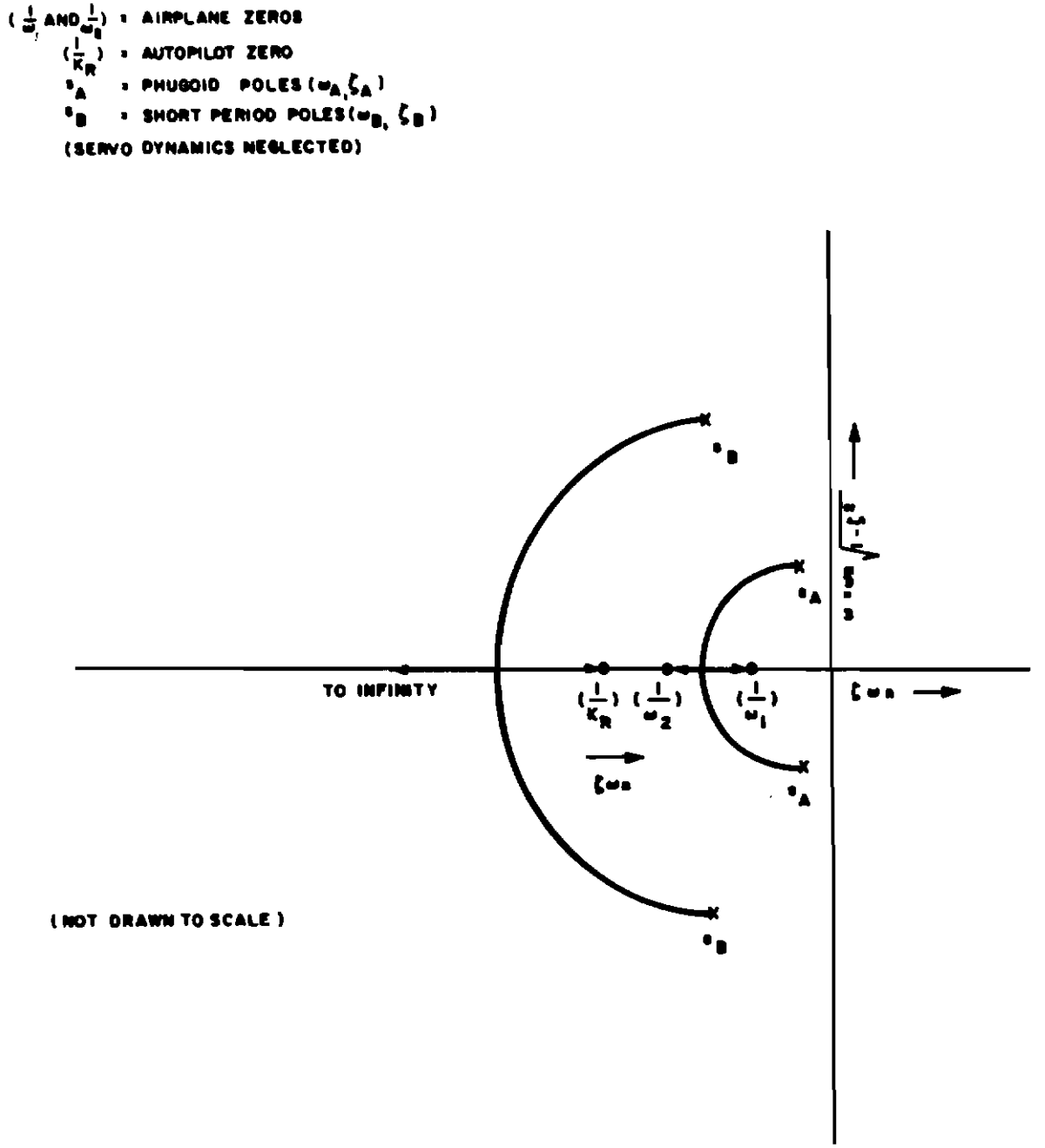

Fig 5

TYPICAL ROOT LOCUS OF
BASIC PITCH ATTITUDE STABILIZATION SYSTEM

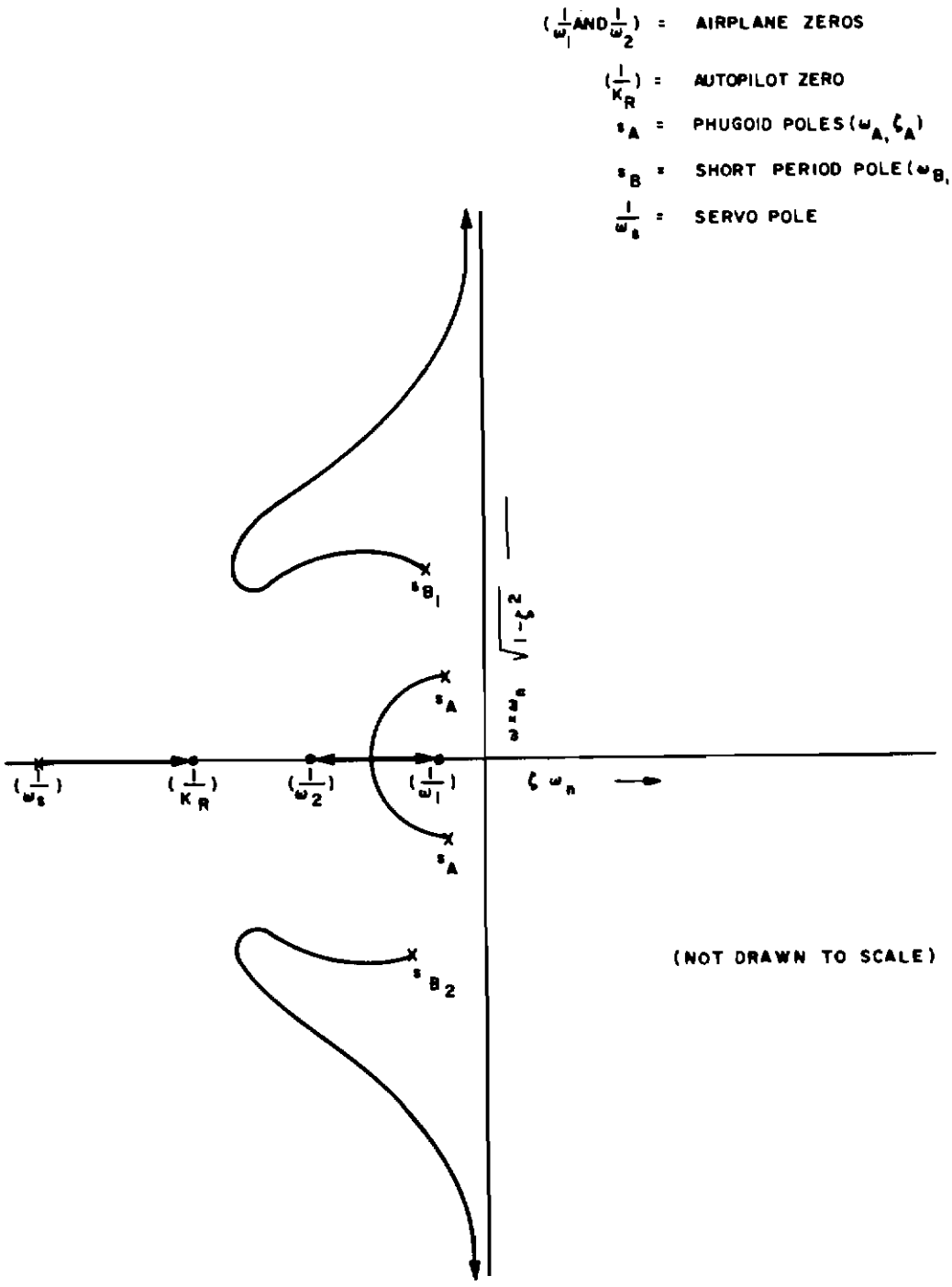

Fig 6

TYPICAL ROOT LOCUS OF PITCH
STABILIZATION SYSTEM WITH IST ORDER SERVO

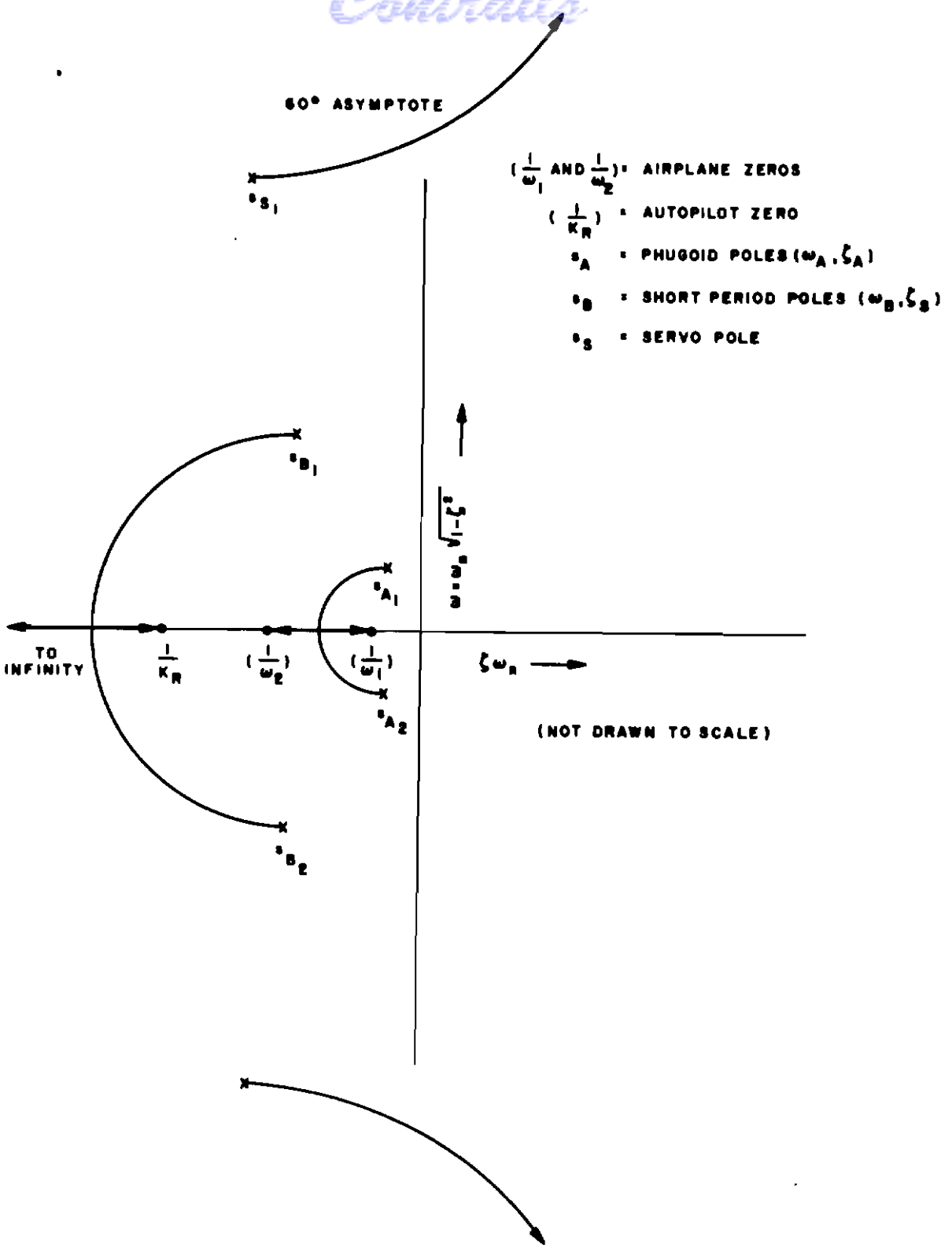

Fig 7

TYPICAL ROOT LOCUS OF PITCH STABILIZATION WITH 2ND ORDER SERVO

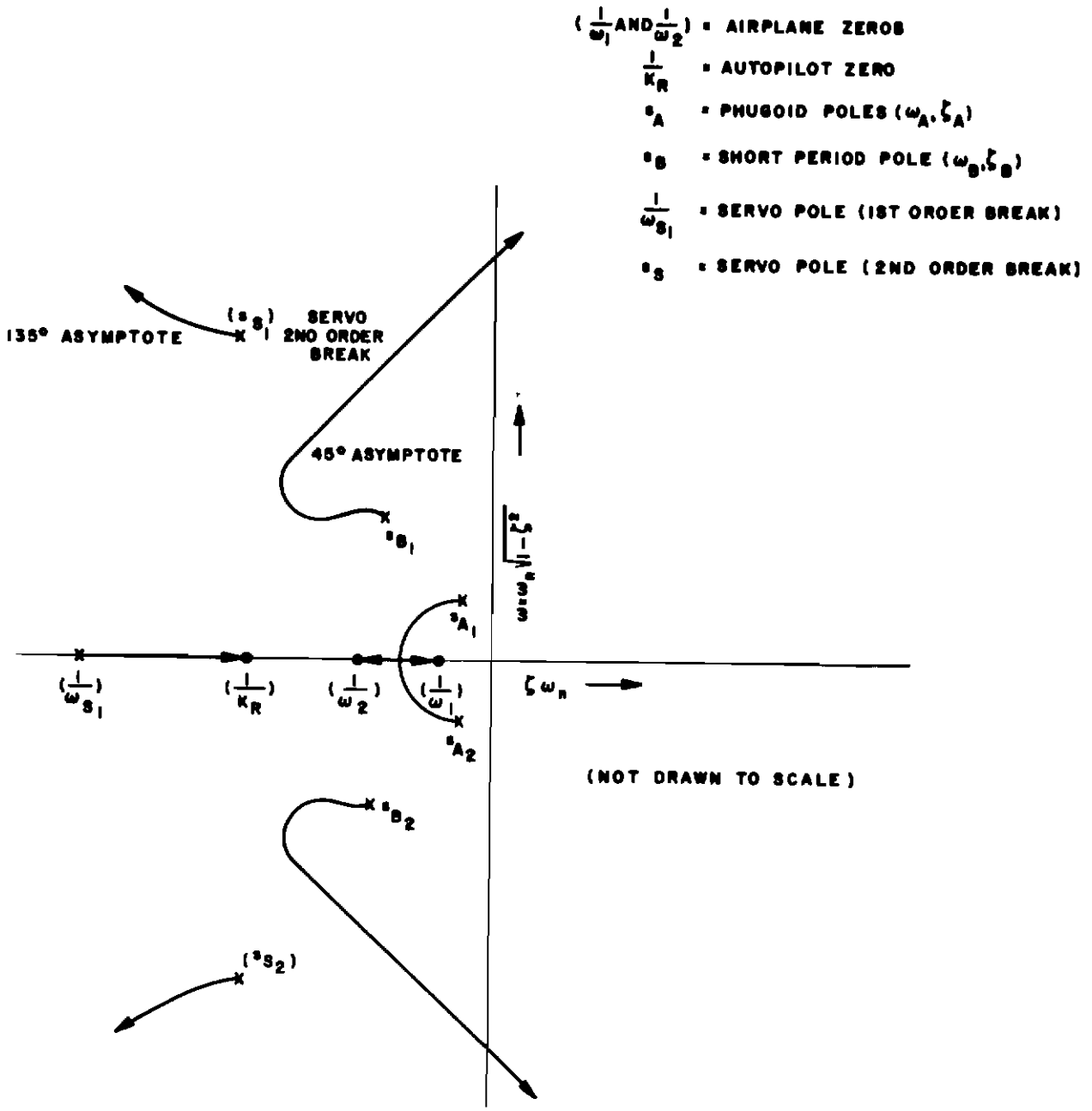

Fig 8

TYPICAL ROOT LOCUS OF
PITCH STABILIZATION
SYSTEM WITH 3RD ORDER SERVO

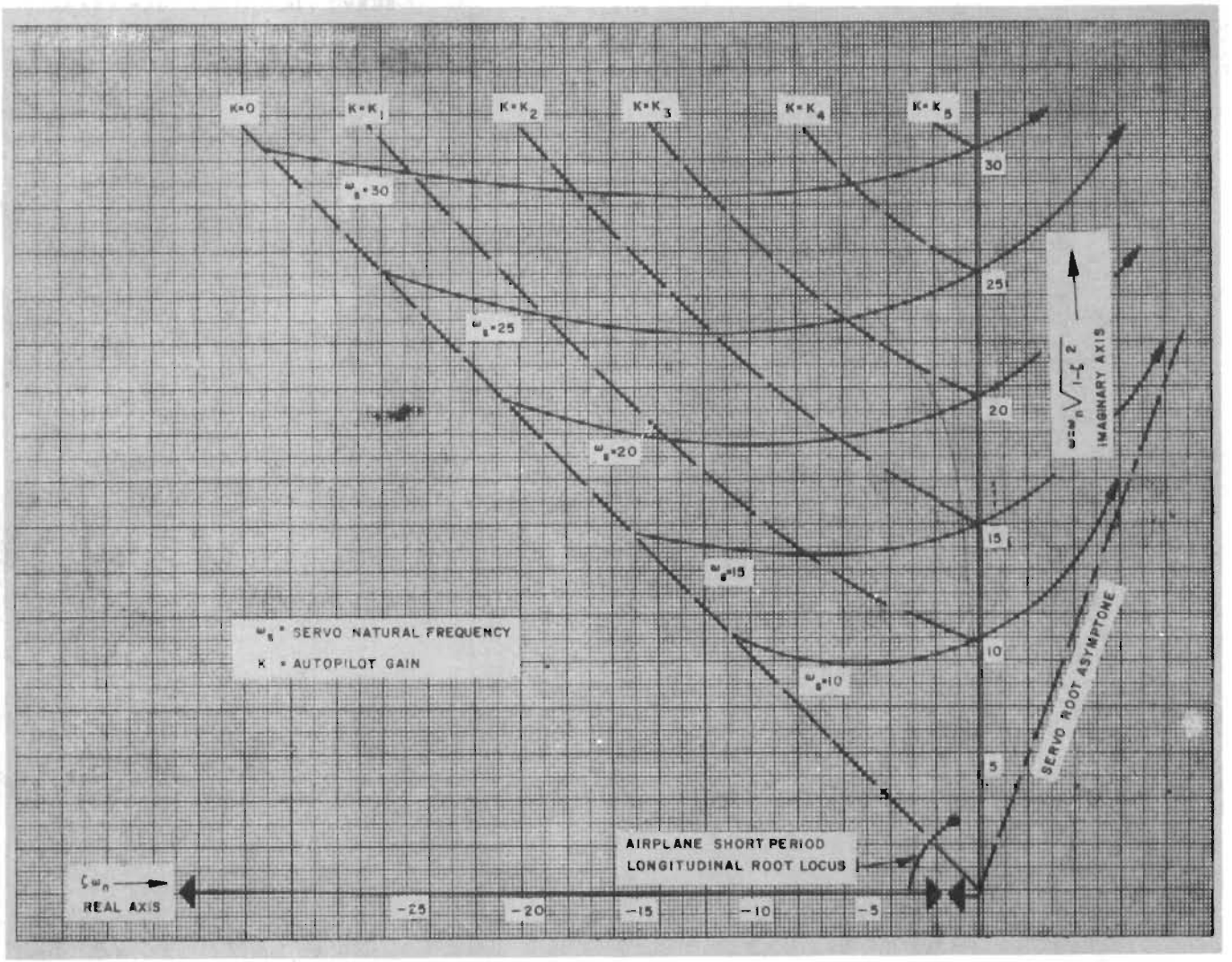

Fig 9

TYPICAL AIRPLANE–AUTOMATIC PILOT LONGITUDINAL ROOT LOCUS WITH 2ND.–ORDER SERVO

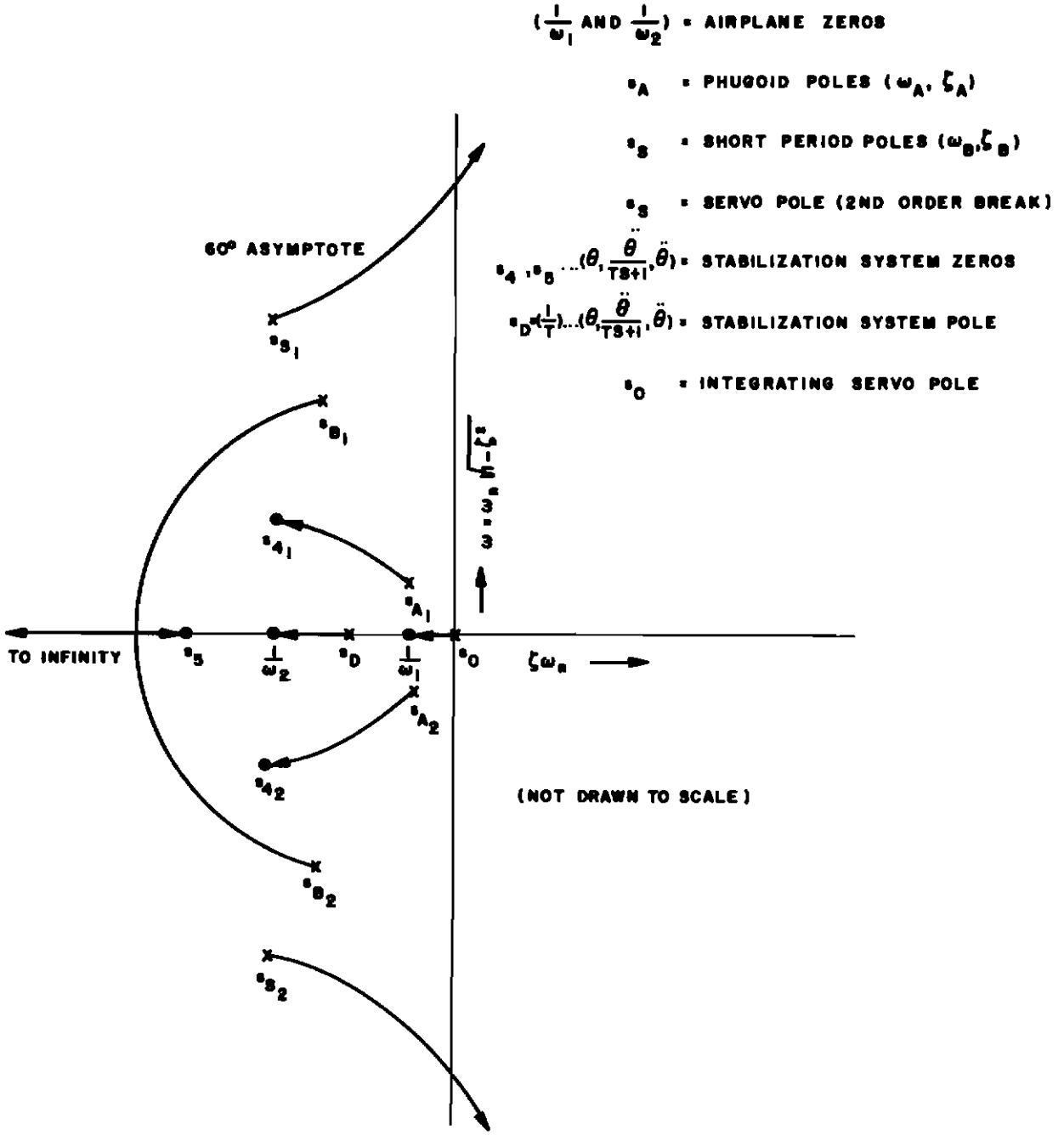

Fig 10

TYPICAL ROOT LOCUS OF PITCH STABILIZATION SYSTEM WITH 3RD ORDER INTEGRATING SERVO

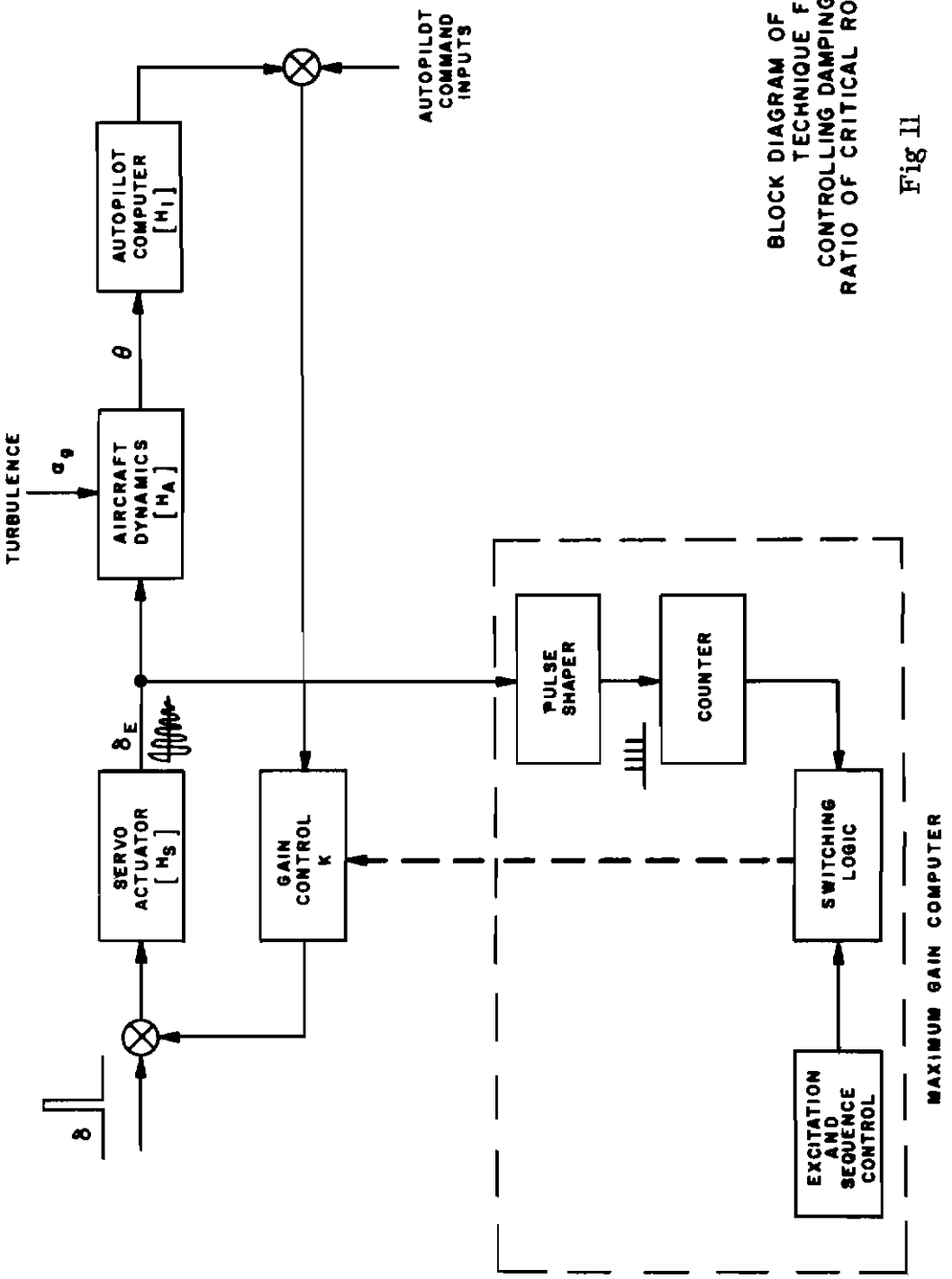

BLOCK DIAGRAM OF TECHNIQUE FOR CONTROLLING DAMPING RATIO OF CRITICAL ROOTS

Fig 11

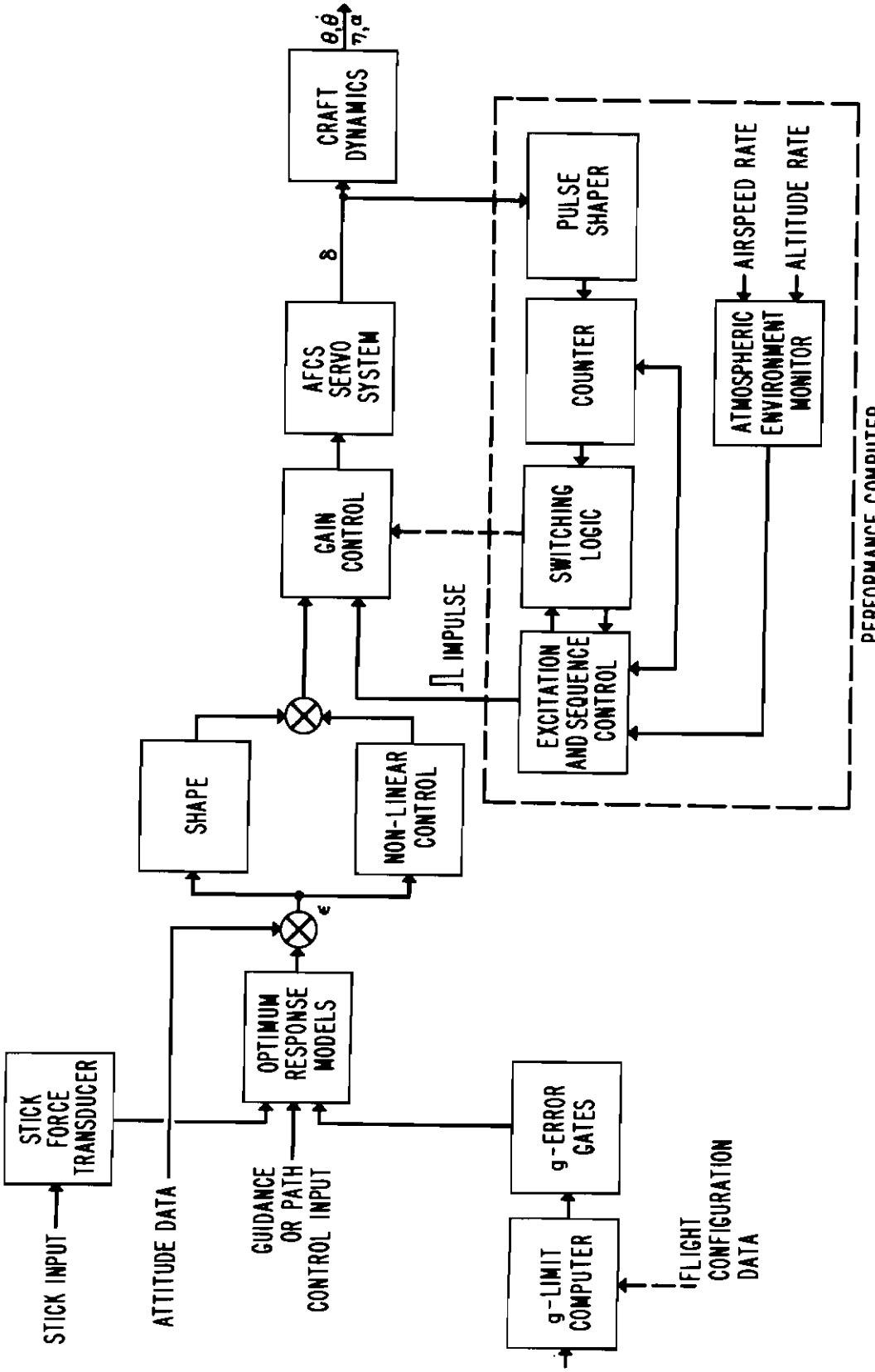

BLOCK DIAGRAM
ADAPTIVE STABILIZATION SYSTEM

Fig 12

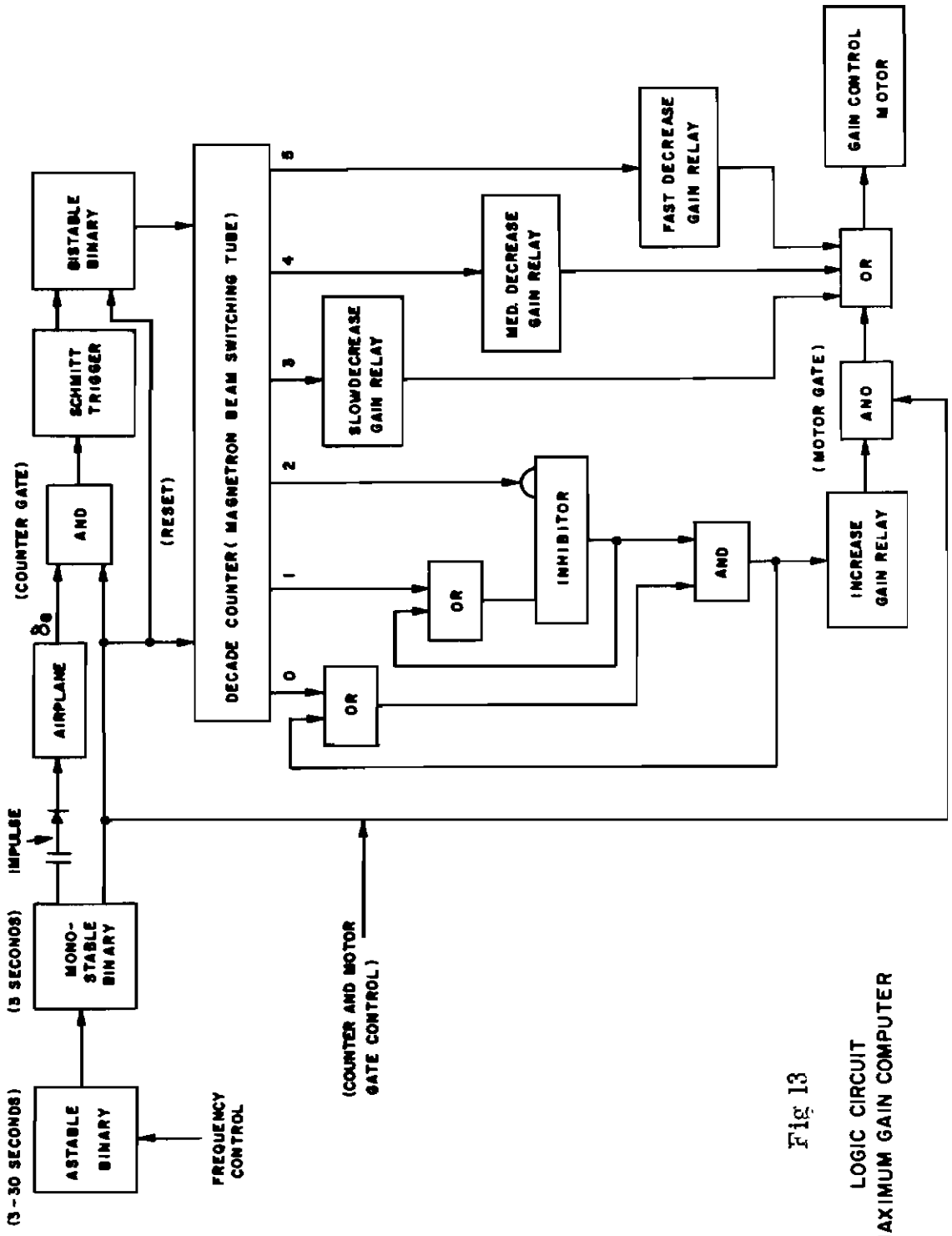

Fig 13

LOGIC CIRCUIT
MAXIMUM GAIN COMPUTER

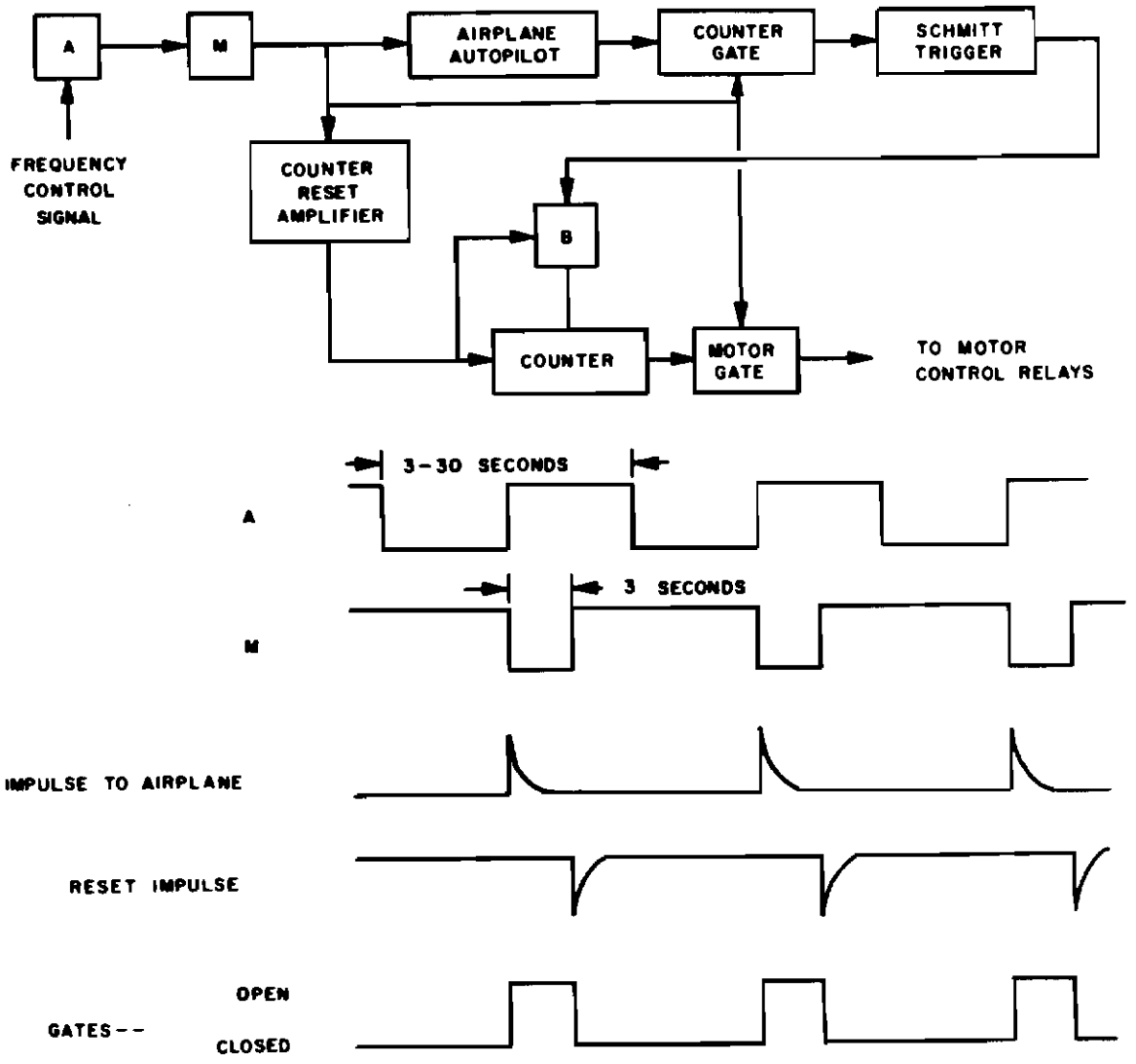

Fig 14

SEQUENCE AND EXCITATION CONTROL BLOCK DIAGRAM

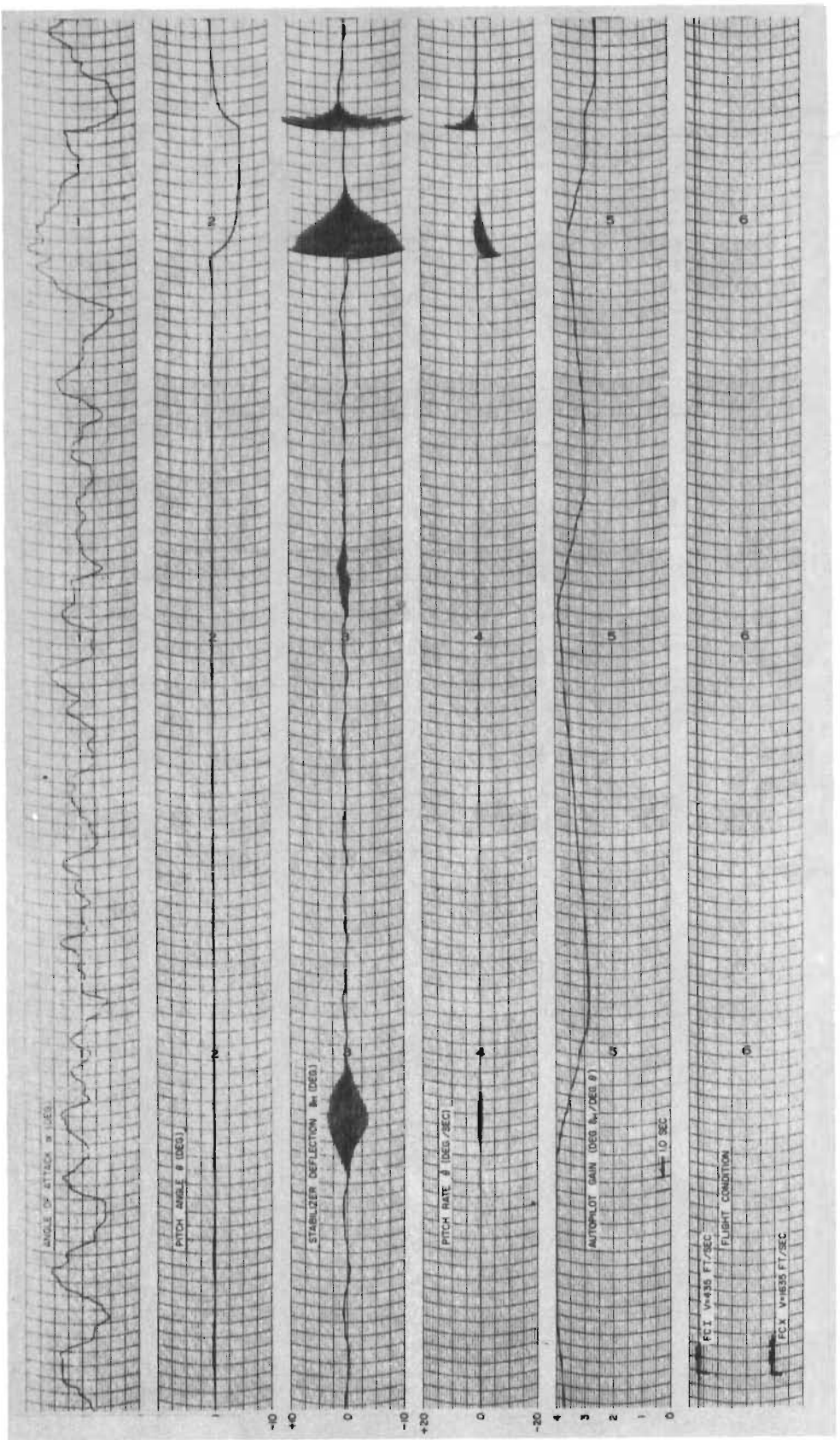

Fig 15

HYPOTHETICAL AIRPLANE-ADAPTIVE AUTOPILOT SYSTEM PERFORMANCE WITH ATMOSPHERIC TURBULENCE AS THE ONLY SOURCE OF EXCITATION

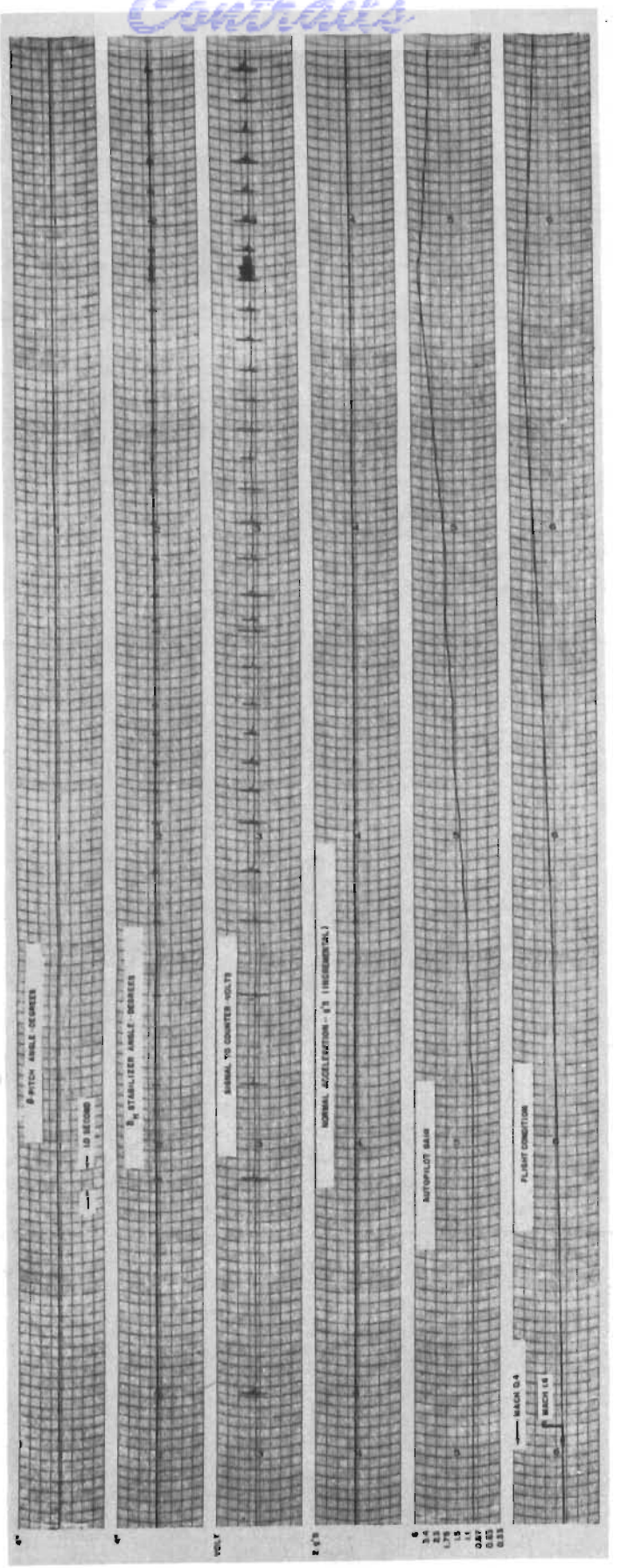

RECORDS OF HYPOTHETICAL AIRPLANE RESPONSE, AUTOPILOT OSCILLATION DURING RECOVERY AND ACCELERATION MANEUVER

Fig 16

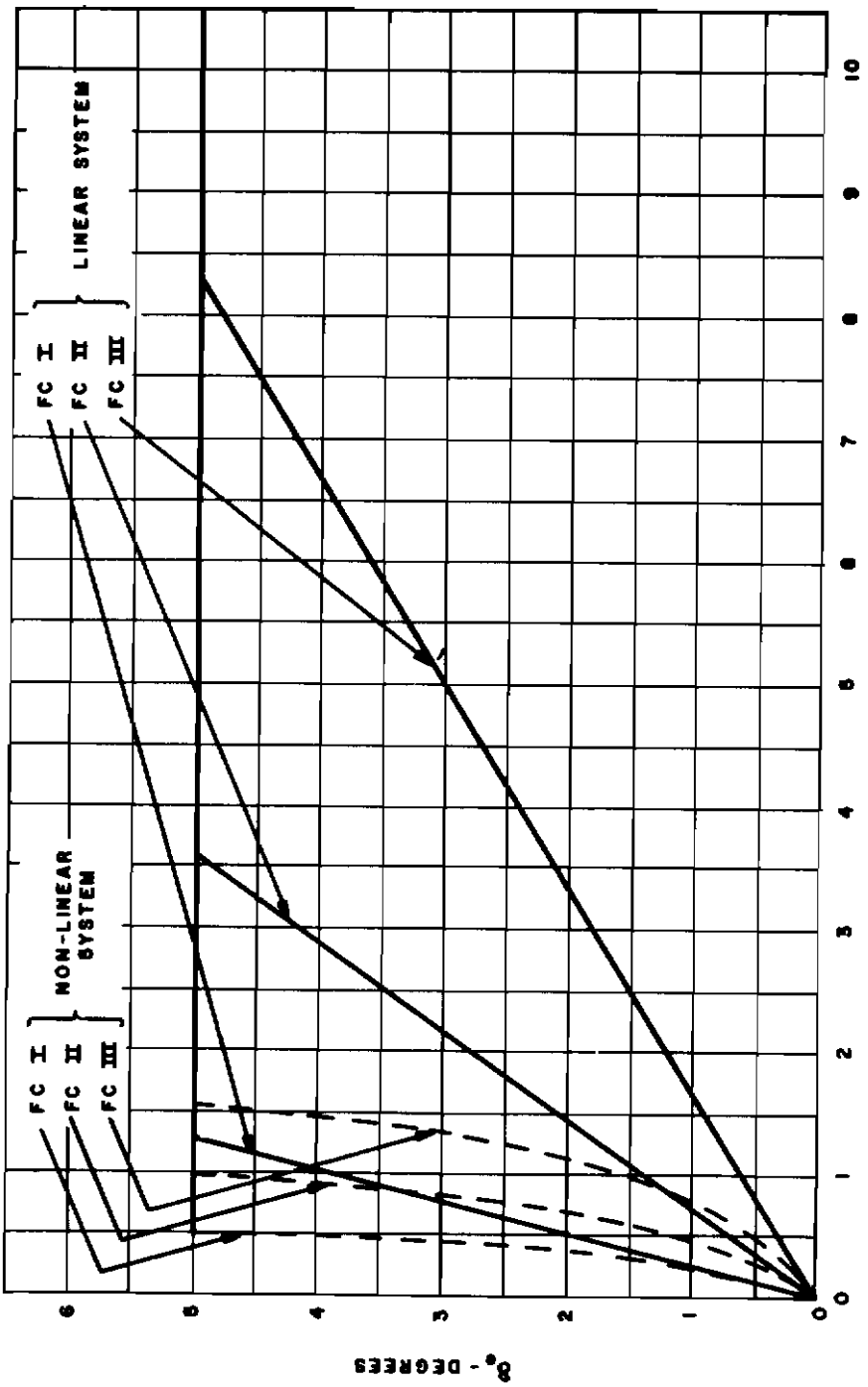

Fig 17
SURFACE DEFELECTION
VS
PITCH ERROR

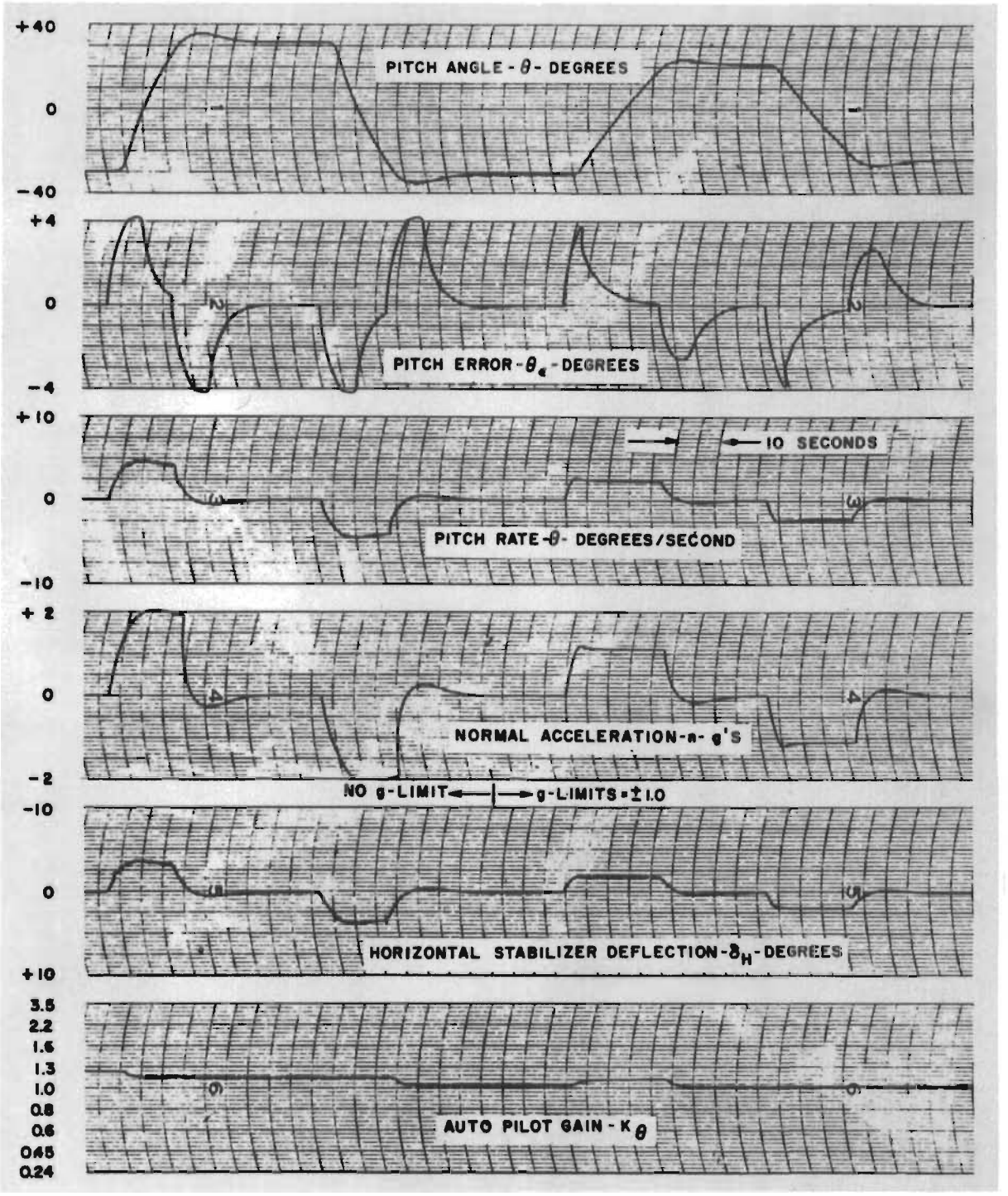

Fig 18

FLIGHT CONDITION II (M=0.95) F104A
PITCH RATE MANEUVERS (2.0g COMMANDS)
WITH AND WITHOUT ±1.0 g - LIMITS
NON-LINEAR ERROR GAIN CONTROLS NOT USED

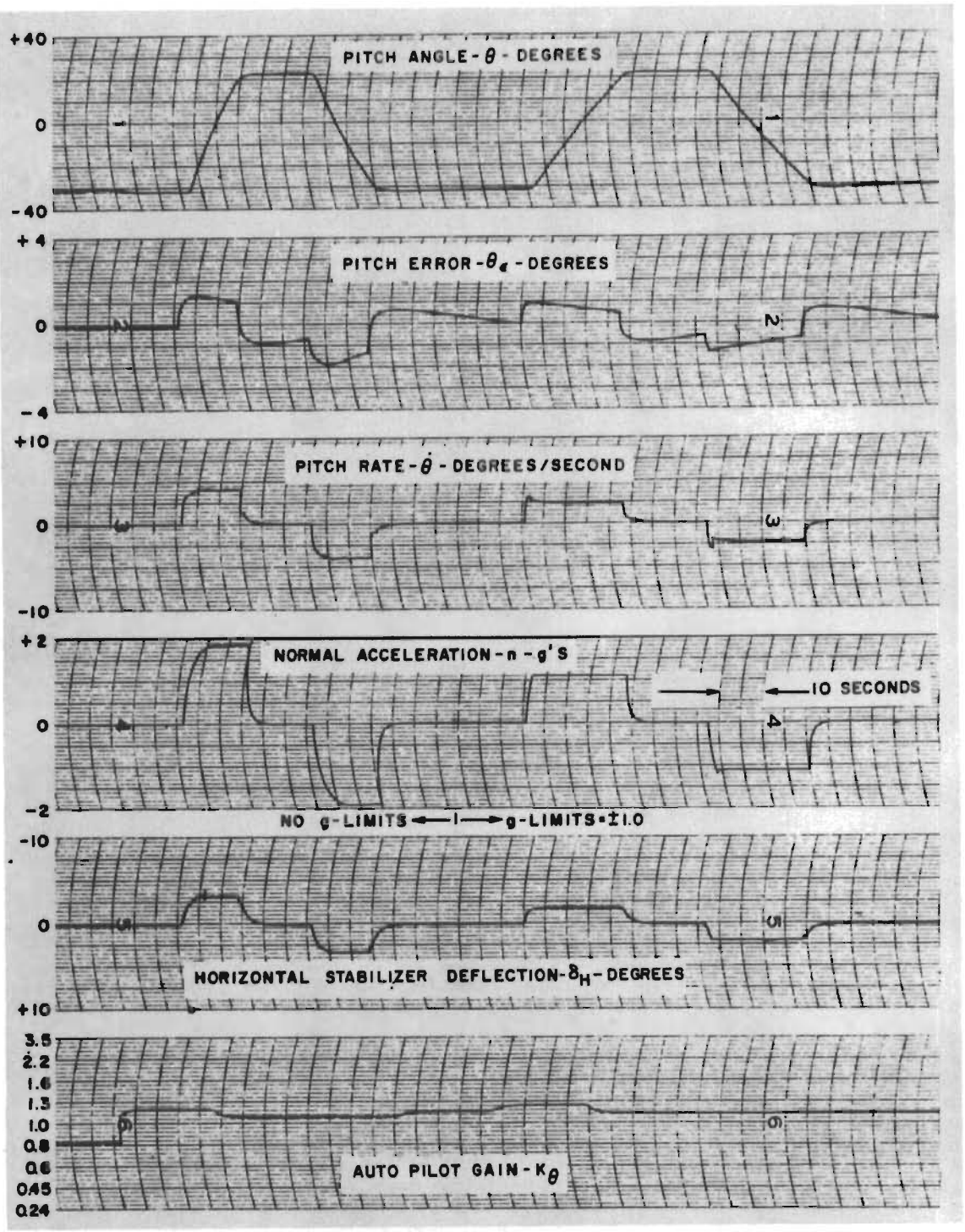

Fig 19

FLIGHT CONDITION II (M=0.95) F104A
PITCH RATE MANEUVERS (2.0g COMMANDS)
WITH AND WITHOUT ± 1.0g - LIMITS
NON-LINEAR ERROR GAIN CONTROLS

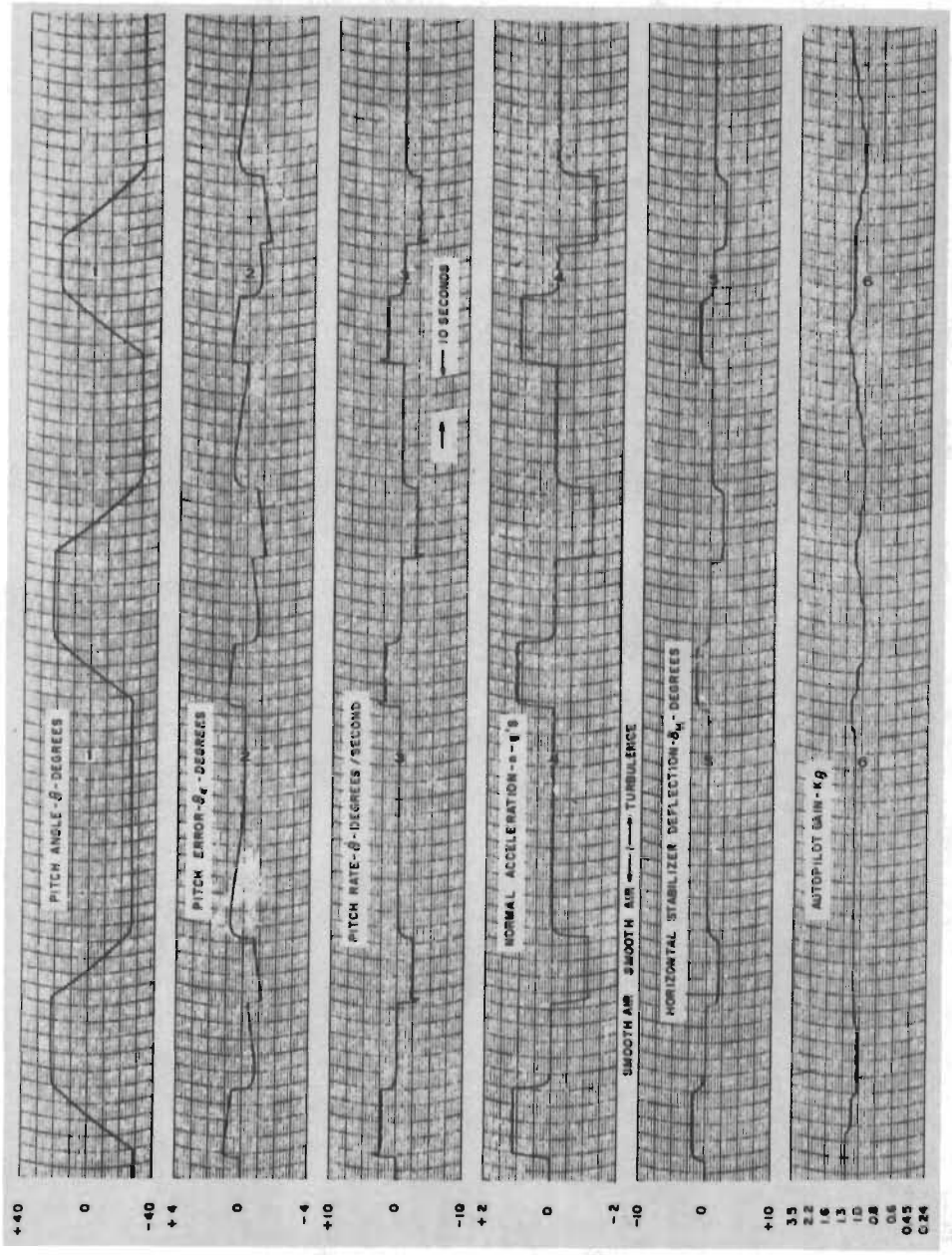

Fig 20

FLIGHT CONDITION II. (M-0.95) F104A
PITCH RATE MANEUVERS (2.0 g-COMMANDS)
IN SMOOTH AND TURBULENT AIR WITH
± LOG-LIMITS AND NON-LINEAR ERROR GAIN CONTROLS

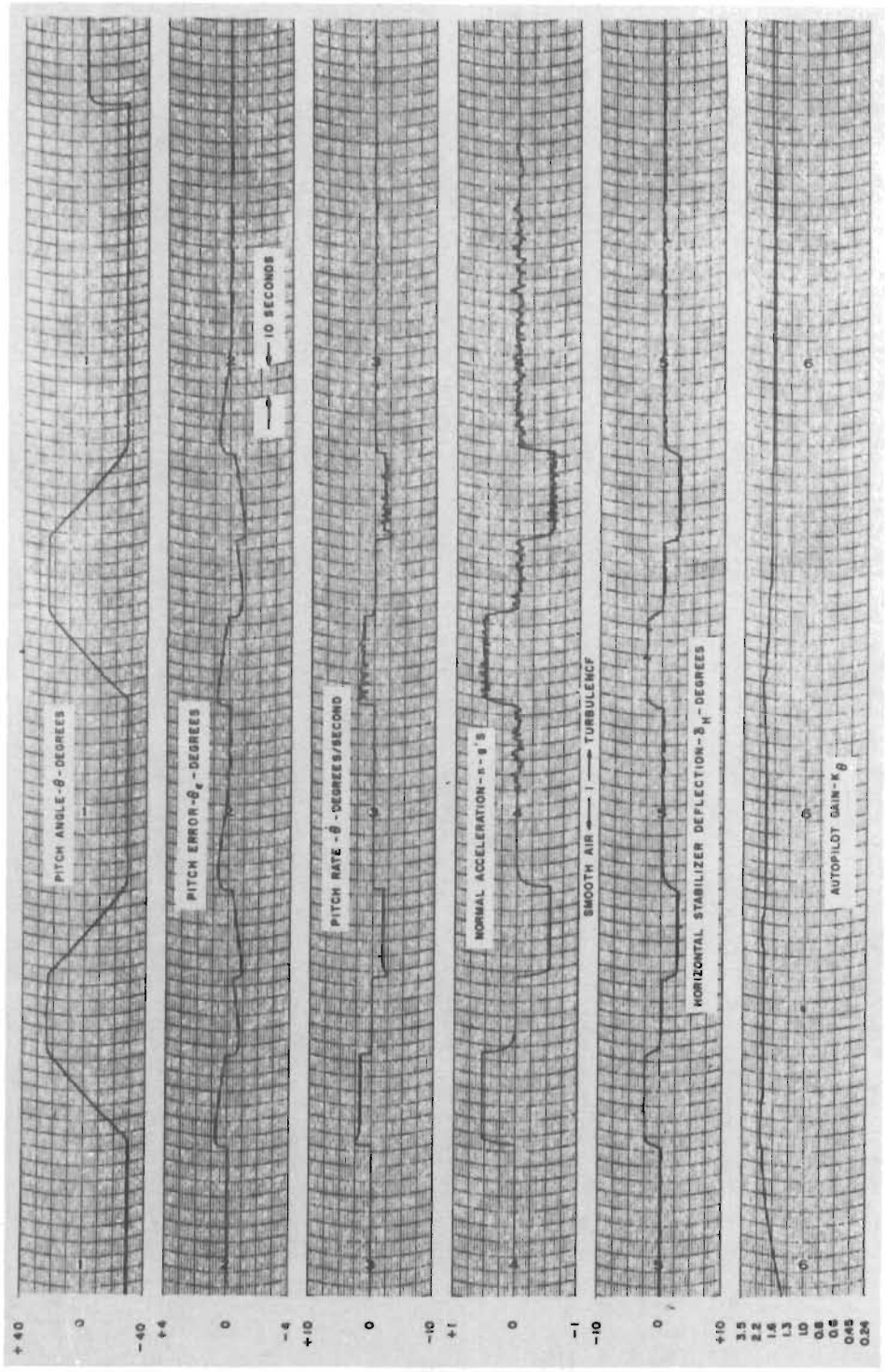

Fig 21

FLIGHT CONDITION II (M=0.6) F104A
PITCH RATE MANEUVERS (1.0 g COMMANDS)
IN SMOOTH AND TURBULENT AIR WITH
±0.5 g LIMITS AND NON-LINEAR ERROR GAIN CONTROLS

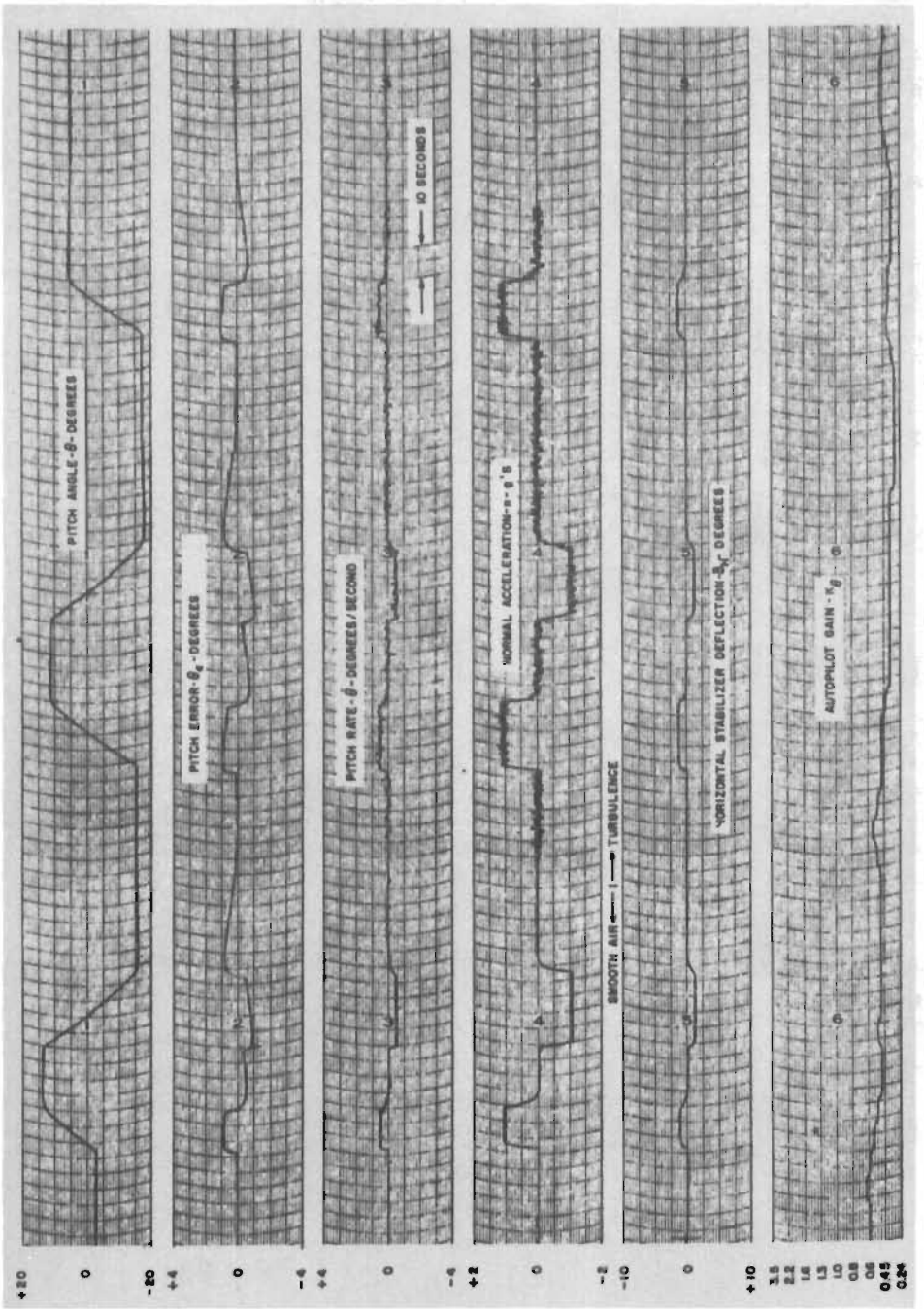

Fig 22

FLIGHT CONDITION III (M-1.6) F104A
PITCH RATE MANEUVERS (2.0g-COMMANDS)
IN SMOOTH AND TURBULENT AIR WITH
±10g-LIMITS AND NON-LINEAR ERROR GAIN CONTROLS

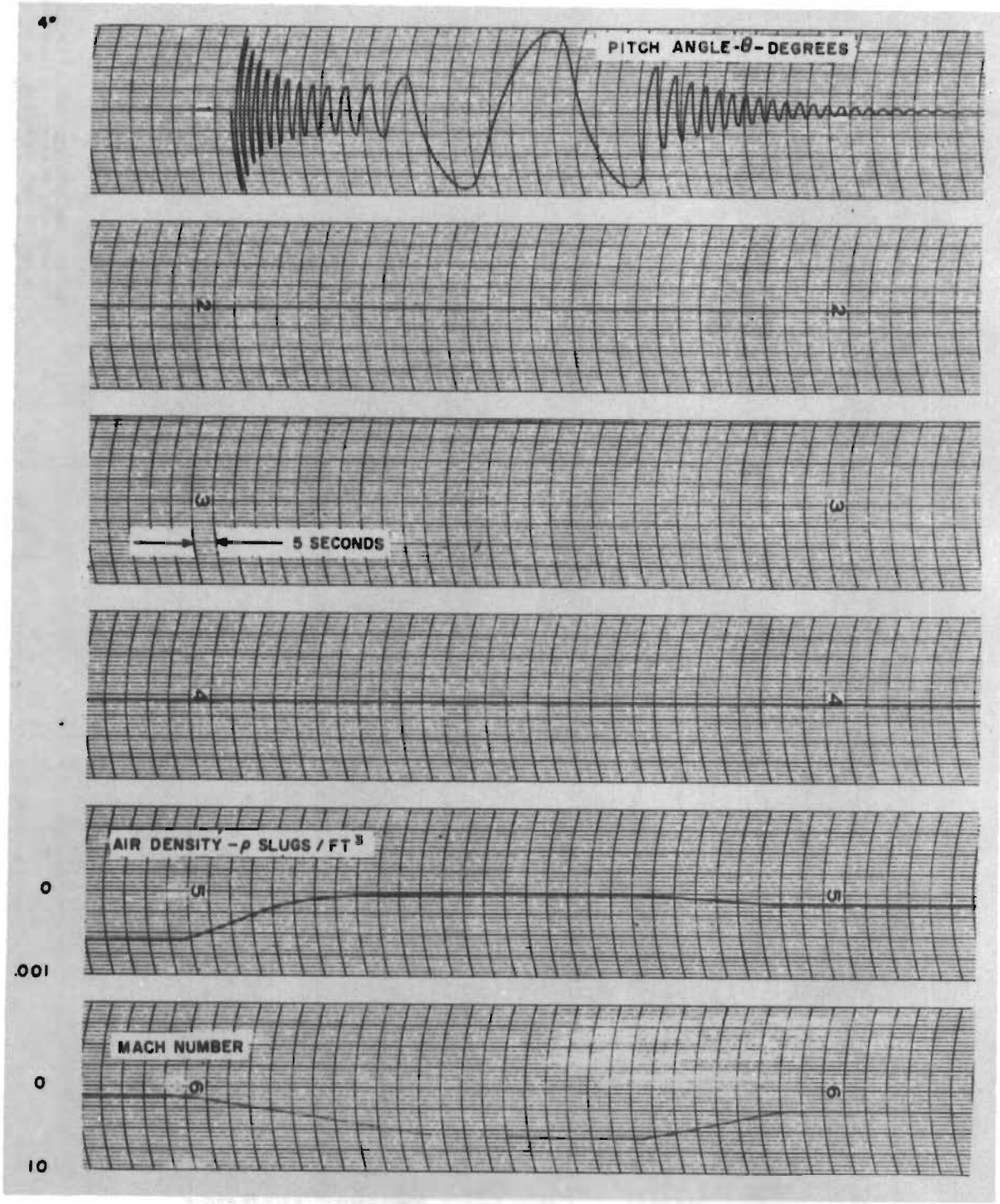

Fig 23

UNCONTROLLED VEHICLE RESPONSE TO DISTURBANCE DURING EXIT AND RE-ENTRY MANEUVER

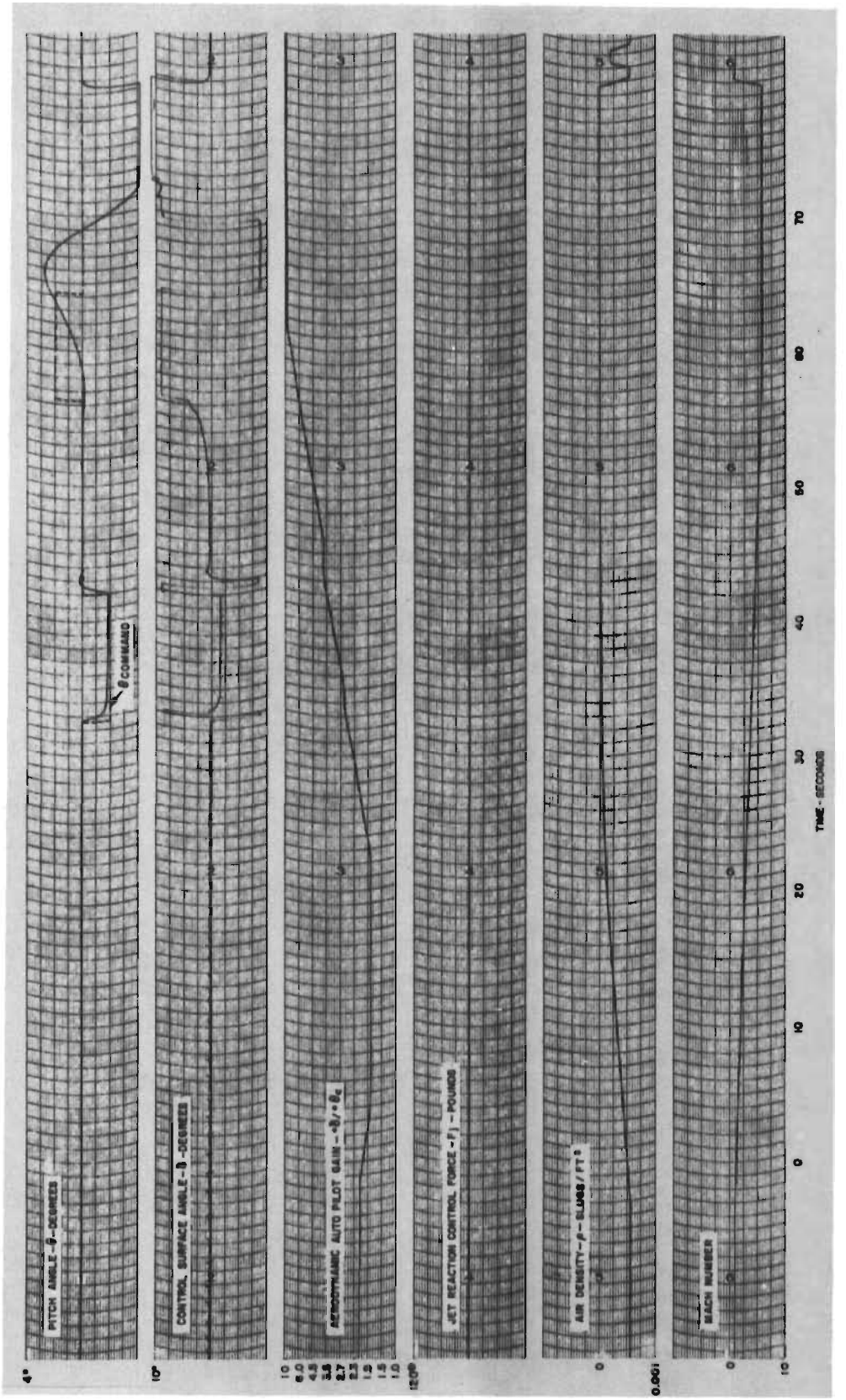

Fig 24

RESPONSE TO 2 DEGREE STEP PITCH COMMANDS DURING EXIT MANEUVER AERODYNAMIC AUTOMATIC PILOT ONLY

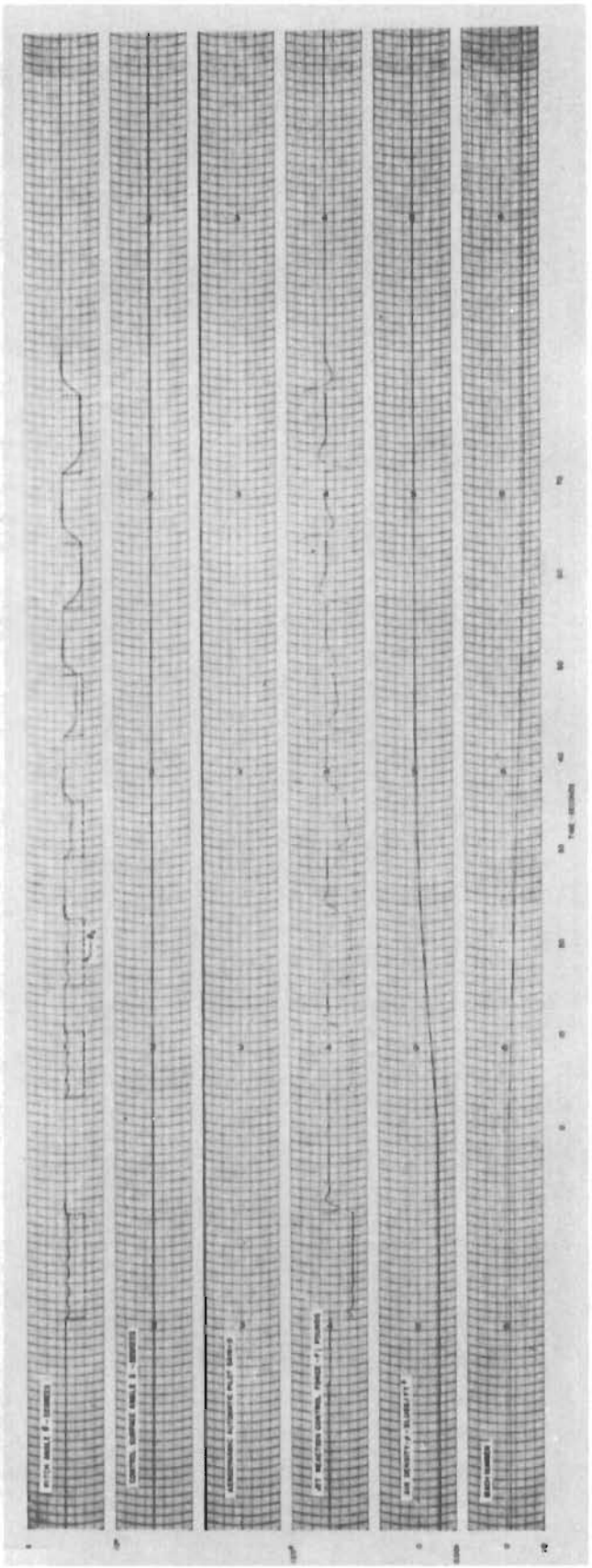

Fig 25

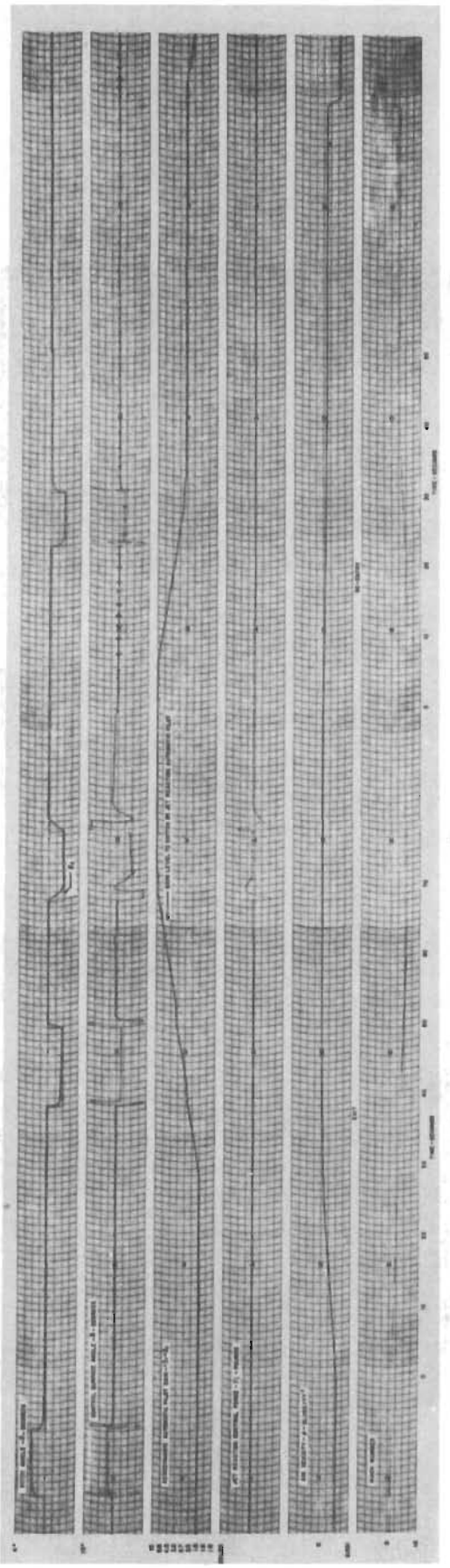

Fig 26

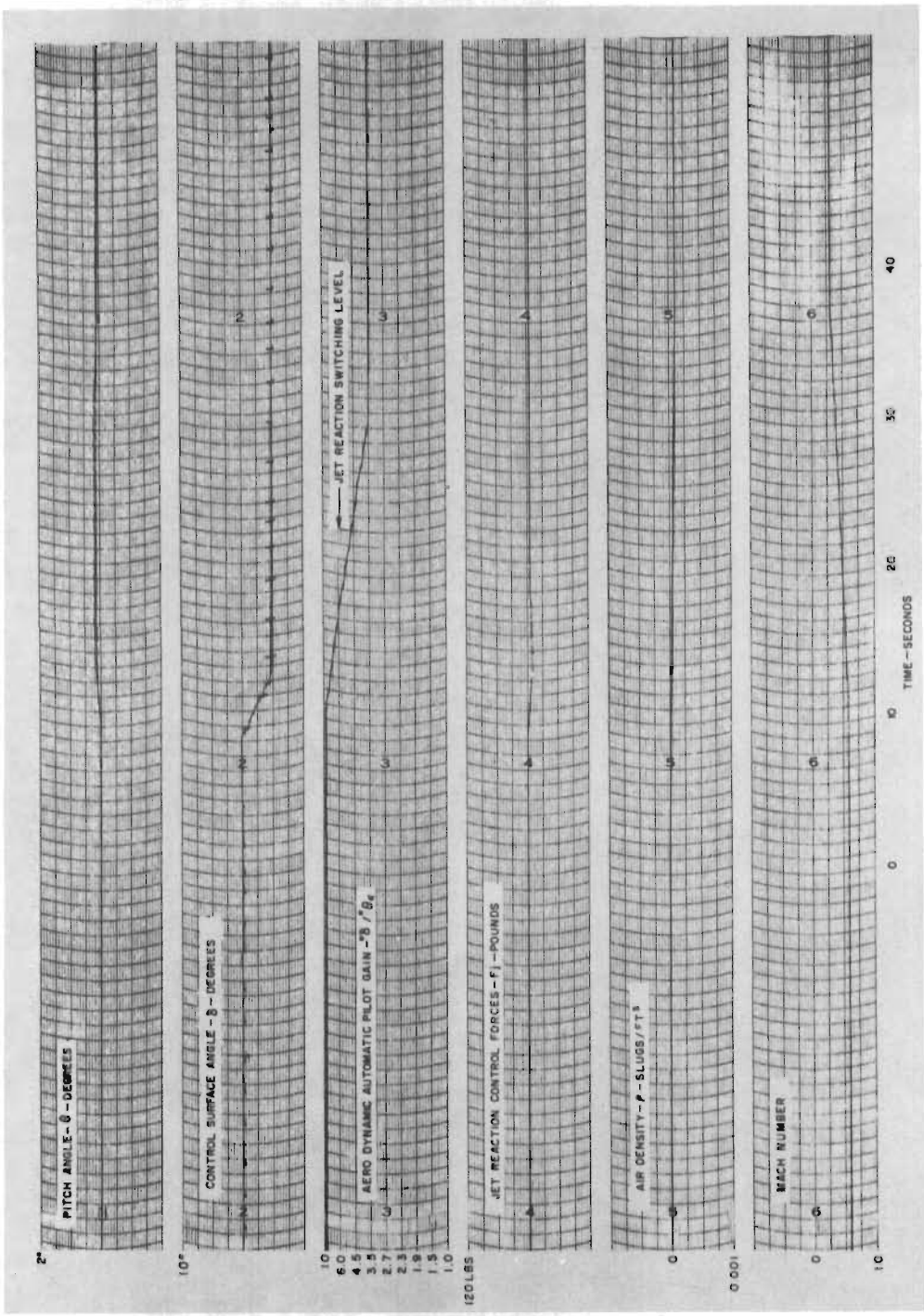

Fig 27

RE-ENTRY MANEUVER WITH CHANGE IN TRIM EQUIVALENT TO FIVE DEGREES OF CONTROL SURFACE OCCURRING IN FOUR SECONDS